$CD11c^+$ cell infiltrations into ablated tumors were lesser in $CCR1^{-/-}$ mice than in WT mice, whereas $F4/80^+$ cells infiltrated RFA-treated tumors in $CCR1^{-/-}$ mice and WT mice to a similar extent (Fig. 4D). These observations suggest that ECI301 augments RFA-induced $CD4^+$, $CD8^+$, and $CD11c^+$ cell infiltrations into RFA-treated tumors in a CCR1-dependent manner.

**ECI301 increases intratumoral expression of CCL3 after RFA**

We showed that $CCR1^+$ cells were mobilized into blood by i.v. administered ECI301. However, the concentration of ECI301 in blood can go down rapidly as time passes (the peak is 5 minutes, and the half-life is <2 hours),[4] allowing ECI301-mobilized $CCR1^+$ cells to migrate into tissues where chemokines are highly produced. To prove this point, chemokine expression in RFA-treated tumors was examined. RFA plus ECI301 treatment increased *CCL3* mRNA expression level 6 hours after RFA. Moreover, 24 hours after treatment, *CCL3* and *CCL4* mRNA expression levels became almost 10-fold higher in tumors treated with RFA alone than in tumors of untreated mice, and ECI301 further increased the mRNA expression level of these chemokines in RFA-treated tumors (Fig. 5A). CCL3 and CCL4 were detected in tumor-infiltrating $F4/80^+$ cells (Fig. 5B). These observations indicate that RFA treatment causes local production of CCL3 and CCL4 in RFA-treated tumors and ECI301 further increases the expression of these chemokines. As the concentration of ECI301 in blood decreases, chemokines produced locally in RFA-treated tumor can attract CCR1-expressing $CD11c^+$ cells, thereby indirectly inducing CCR1-negative $CD4^+$ and $CD8^+$ cell infiltrations.

**ECI301 augments RFA-induced tumor-specific immune responses accompanied by T-cell infiltrations into non–RFA-treated tumors**

Non–RFA-treated tumors were analyzed histologically to clarify the mechanisms underlying the CCR1-dependent inhibitory effect of RFA plus ECI301 treatment against these tumors. Although few $CD4^+$ or $CD8^+$ cells were observed in the tumors of untreated mice, RFA treatment increased the numbers of $CD4^+$ and $CD8^+$ cells in the non–RFA-treated tumors 3 days after RFA. ECI301 further augmented RFA-induced $CD4^+$ and $CD8^+$ cell infiltrations into non–RFA-treated tumors (Fig. 6A and B). However, only a marginal number of $CD11c^+$ or $F4/80^+$ cells infiltrated into non–RFA-treated tumors of mice treated with RFA alone or RFA plus ECI301-treated mice (data not shown). Based on these findings, we hypothesized that ECI301-augmented tumor regression after RFA may be associated with T-cell–mediated antitumor immune responses. To clarify this point, *nu/nu* mice on a BALB/c background were treated by RFA with or without ECI301. Deficiency of T cells abrogated the tumor-inhibitory effect of ECI301 as well as the RFA-induced antitumor effect (Fig. 6C). Thus, both ECI301- and RFA-induced tumor regressions require T-cell–mediated antitumor immune response.

[4] Unpublished data from Effector Cell Institute.

However, $CD4^+$ or $CD8^+$ T cells rarely expressed CCR1 in blood and RFA-treated tumors. $CCR1^+$ cells in RFA-treated tumors were $CD11c^+$ cells and $F4/80^+$ cells, and only the former accumulate in RFA-treated tumors in a CCR1-dependent manner. These findings suggest that CCR1-positive $CD11c^+$ cells may activate antitumor T-cell responses and indirectly induce tumor retardation. Accordingly, we next examined the effect of depletion of monocytes/macrophages on ECI301-augmented tumor regression. I.p. injection of clodronate liposome depleted CD11c-negative monocytes in blood, although it did not change the number of $CD11c^+$ cells (data not shown). Depletion of these CD11c-negative monocytes did not cause any effects on ECI301-enhanced tumor regression, indicating that ECI301-augmented antitumor T-cell immunity was independent of CD11c-negative monocytes (Fig. 6C).

Finally, to prove the presence of systemic adaptive immune responses, IFN-γ ELISPOT assay was performed using mononuclear cells from the spleen. A greater number of spots against BNL cell lysates, but not against CT26 cell lysates, were generated by RFA plus ECI301–treated mice than that by mice treated with RFA alone or untreated mice. Moreover, ablation of *CCR1* gene, but not *CCR5* gene, reduced the number of spots against BNL cell lysates even when the mice were treated with RFA plus ECI301 (Fig. 6D). These observations suggest that ECI301 can further augment RFA-induced tumor-specific adaptive immune responses and subsequent tumor retardation in a CCR1-dependent manner.

## Discussion

HCC occurs predominantly in individuals with chronic liver disease related to hepatitis B or hepatitis C virus infections (22–24). In addition to surgical resection, RFA treatment has been developed to eradicate solitary HCC lesions (25). RFA of HCC induces specific T-cell responses against liver tumors in human and rabbit (8, 11). Moreover, activated dendritic cells were detected in peripheral blood of HCC patients after RFA (9). These previous reports indicate that RFA treatment can induce antitumor immune responses against HCC (8–11). Likewise, we observed that RFA treatment generated tumor-specific IFN-γ–producing cells and inhibited the growth of non–RFA-treated tumors accompanied by massive T-cell infiltration into these tumors. However, even after successful ablation of HCC lesion by RFA, tumor recurrence often occurs probably because HCC develops in a multicentric manner in the cirrhotic liver (12). These observations indicate that RFA-induced augmentation in immune response may not be sufficient to prevent tumor recurrence. Thus, a novel therapeutic modality is required to further augment RFA-induced tumor-specific immune responses. Here, we showed that combined administration of ECI301 and RFA can augment tumor-specific immune responses against HCC.

Several chemokines are used for immunotherapy against cancers because they can attract immune cells such as dendritic and cytotoxic T cells to augment tumor-specific immune responses (26). However, some chemokines can simultaneously attract myeloid-derived suppressor and regulatory T cells to promote neovascularization and induce immunosuppressive

microenvironments (26–28). The double-edged activities of chemokines frequently preclude their use for tumor immunotherapy. Moreover, most chemokines exhibit a bell-shaped dose-response curve with a narrow effective dose window. Thus, determination of an optimal dose of chemokines is important to elicit efficient antitumor responses (29). Several lines of evidence show that intratumoral use of CCL3 reduces tumorigenicity (6, 30). Furthermore, there are no reports showing that use of CCL3 can promote tumor progression. We observed that systemic administration of ECI301 without RFA treatment induced neither reduction nor progression of tumors. On the contrary, systemic injection of ECI301 after RFA can inhibit the growth of non–RFA-treated tumors in the contralateral side. ECI301-enhanced tumor regression after RFA was both CCR1 and T-cell dependent, but T cells rarely expressed CCR1 in blood and RFA-treated tumors. Because depletion of monocytes/macrophages did not affect the retardation of ECI301-treated tumors, CCR1-expressing $CD11c^+$ dendritic cells might activate antitumor T-cell responses and indirectly induce tumor retardation via some mechanisms such as antigen presentation and cytokine production. ECI301 mobilized a large number of $CCR1^+$ cells into blood, and these mobilized cells may be attracted into highly CCL3-producing RFA-treated tumors and cause increased number of tumor-infiltrating $CCR1^+CD11c^+$ dendritic cells. Thus, $CCR1^+$ precursors in blood and $CCR1^+CD11c^+$ tumor-infiltrating dendritic cells might play important roles in ECI301-augmented antitumor effects (31–33).

ECI301 could not increase the number of $F4/80^+$ cells in the RFA-treated tumor sites. Accumulation of $F4/80^+$ cells in the tumor treated with ECI301 plus RFA was also independent of CCR1. $F4/80^+$ cells, which might include a large number of macrophages/monocytes, are usually attracted into the tumor by CCL2, CCL4, and CCL5 that are produced in the tumor sites. CCR2, the receptor for CCL2, and CCR5, the receptor for CCL4 and CCL5, might be responsible for migration of monocytes/macrophages (27, 34–36). However, it is still unclear whether monocytes/macrophages use CCR2 or CCR5 after massive tumor cell death caused by treatments such as RFA because tumor cell death induces different profiles of chemokine production in the tumors (4). Although ECI301 did not directly induce migration of $F4/80^+$ cells, the mechanism underlying the infiltration of $F4/80^+$ macrophages remains to be elucidated.

Breaking tolerance for tumor cells is necessary for induction of antitumor immunity. Several independent groups have suggested multiple mechanisms underlying immunogenic tumor cell death induced by anticancer chemotherapy or radiation therapy (37–40). Anthracyclin causes apoptosis along with translocation of calreticulin to the apoptotic tumor cell surface. Calreticulin exposure augments phagocytosis of apoptotic cancer cells by dendritic cells with an eventual increase in immune response (37, 38). Chemotherapy or irradiation kills tumor cells to release high mobility group box 1 (HMGB1). Released HMGB1 activates dendritic cells after binding to toll-like receptor 4 expressed by these cells (39). Apoptosis induced by local radiation therapy augments MHC class I expression by tumor cells, thereby facilitating their recognition by cytotoxic T cells (40). RFA induces the expression of heat shock proteins 70 and 90 on ablated tumor cells, and these proteins can activate toll-like receptor–expressing antigen-presenting cells (41, 42). In addition, we showed that RFA treatment alone caused local production of CCL3 in RFA-treated tumors accompanied by accumulation of T cells and $CD11c^+$ dendritic cells. These mechanisms may also account for the observed RFA-induced generation of tumor-specific immune responses.

We revealed that combined treatment of ECI301 and RFA augmented antitumor-specific immune responses, thereby inhibiting the growth of non–RFA-treated tumors in a CCR1-dependent manner. Thus, combined treatment of ECI301 and RFA can prevent human HCC from recurring after RFA treatment. The absence of any severe adverse effects in mice (data not shown) further warrants the clinical trial of ECI301 combined with RFA as a treatment regimen for HCC.

## Disclosure of Potential Conflicts of Interest

No potential conflicts of interest were disclosed.

## Acknowledgments

We thank Dr. Philip M. Murphy (National Institute of Allergy and Infectious Disease, NIH) and Dr. Kouji Matsushima (Tokyo University) for providing us with $CCR1^{-/-}$ and $CCR5^{-/-}$ mice, respectively.

The costs of publication of this article were defrayed in part by the payment of page charges. This article must therefore be hereby marked *advertisement* in accordance with 18 U.S.C. Section 1734 solely to indicate this fact.

Received 01/11/2010; revised 06/01/2010; accepted 06/20/2010; published OnlineFirst 07/27/2010.

## References

1. Luster AD. Chemokines—chemotactic cytokines that mediate inflammation. N Engl J Med 1998;338:436–45.
2. Castellino F, Huang AY, Altan-Bonnet G, Stoll S, Scheinecker C, Germain RN. Chemokines enhance immunity by guiding naïve $CD8^+$ T cells to sites of $CD4^+$ T cell-dendritic cell interaction. Nature 2006;440:890–5.
3. Sozzani S. Dendritic cell trafficking: more than just chemokines. Cytokine Growth Factor Rev 2005;16:581–92.
4. Iida N, Nakamoto Y, Baba T, et al. Tumor cell apoptosis induces tumor-specific immunity in a CC chemokine receptor 1-and 5-dependent manner in mice. J Leukoc Biol 2008;84:1001–10.
5. Tsuchiyama T, Nakamoto Y, Sakai Y, et al. Prolonged, NK cell-mediated antitumor effects of suicide gene therapy combined with monocyte chemoattractant protein-1 against hepatocellular carcinoma. J Immunol 2007;178:574–83.
6. Crittenden M, Gough M, Harrington K, Olivier K, Thompson J, Vile RG. Expression of inflammatory chemokines combined with local tumor destruction enhances tumor regression and long-term immunity. Cancer Res 2003;63:5505–12.
7. Furumoto K, Soares L, Engleman EG, Merad M. Induction of potent antitumor immunity by *in situ* targeting of intratumoral DCs. J Clin Invest 2004;113:774–83.

8. Zerbini A, Pilli M, Penna A, et al. Radiofrequency thermal ablation of hepatocellular carcinoma liver nodules can activate and enhance tumor-specific T-cell responses. Cancer Res 2006;66:1139–46.
9. Ali MY, Grimm CF, Ritter M, et al. Activation of dendritic cells by local ablation of hepatocellular carcinoma. J Hepatol 2005;43:817–22.
10. Brok MH, Sutmuller RP, Voort R, et al. *In situ* tumor ablation creates antigen source for the generation of antitumor immunity. Cancer Res 2004;64:4024–9.
11. Wissniowski TT, Hünsler J, Neureiter D, et al. Activation of tumor-specific T lymphocytes by radio-frequency ablation of the VX2 hepatoma in rabbits. Cancer Res 2003;63:6496–500.
12. Poon RT, Fan ST, Ng IO, Lo CM, Liu CL, Wong J. Different risk factors and prognosis for early and late intrahepatic recurrence after resection of hepatocellular carcinoma. Cancer 2000;89:500–7.
13. Hunter MG, Bawden L, Brotherton D, et al. BB-10010: an active variant of human macrophage inflammatory protein-1α with improved pharmaceutical properties. Blood 1995;86:4400–8.
14. Clemons MJ, Marshall E, Dürig J, et al. A randomized phase-II study of BB-10010 (macrophage inflammatory protein-1α) in patients with advanced breast cancer receiving 5-fluorouracil, Adriamycin, and cyclophosphamide chemotherapy. Blood 1998;92:1532–40.
15. Zhang Y, Yoneyama H, Wang Y, et al. Mobilization of dendritic cell precursors into the circulation by administration of MIP-1α in mice. J Natl Cancer Inst 2004;96:201–9.
16. Taub DD, Conlon K, Lloyd AR, Oppenheim JJ, Kelvin DJ. Preferential migration of activated $CD4^+$ and $CD8^+$ T cells in response to MIP-1α and MIP-1β. Science 1993;260:355–8.
17. Shiraishi K, Ishiwata Y, Nakagawa K, et al. Enhancement of antitumor radiation efficacy and consistent induction of the abscopal effect in mice by ECI301, an active variant of macrophage inflammatory protein-1α. Clin Cancer Res 2008;14:1159–66.
18. Isoai A, Kimura H, Reichert A, et al. Production of D-amino acid oxidase of *Trigonopsis variabilis* in *Schizosaccharomyces pombe* and the characterization of biocatalysts prepared with recombinant cells. Biotechnol Bioeng 2002;80:22–32.
19. Lu P, Nakamoto Y, Nemoto-Sakai Y, et al. Potential interaction between CCR1 and its ligand, CCL3, induced by endogeneously produced interleukin-1 in human hepatomas. Am J Pathol 2003;162:1249–58.
20. Lu P, Li L, Liu G, Rooijen N, Mukaida N, Zhang X. Opposite roles of CCR2 and CX3CR1 macrophages in alkali-induced corneal neovascularization. Cornea 2009;28:562–9.
21. Sadahira Y, Yasuda T, Yoshino T, et al. Impaired splenic erythropoiesis in phlebotomized mice injected with CL2MDP-liposome: an experimental model for studying the role of stromal macrophages in erythropoiesis. J Leukoc Biol 2000;68:464–70.
22. Tsukuma H, Hiyama T, Tanaka S, et al. Risk factors for hepatocellular carcinoma among patients with chronic liver disease. N Engl J Med 1993;328:1797–801.
23. Velázquez RF, Rodríguez M, Navascués CA, et al. Prospective analysis of risk factors for hepatocellular carcinoma in patients with liver cirrhosis. Hepatology 2003;37:520–7.
24. Okita K. Management of hepatocellular carcinoma in Japan. J Gastroenterol 2006;41:100–6.
25. Tateishi R, Shiina S, Ohki T, et al. Treatment strategy for hepatocellular carcinoma: expanding the indication for radiofrequency ablation. J Gastroenterol 2009;44 Suppl:142–6.
26. Homey B, Müller A, Zlotnik A. Chemokines: agents for the immunotherapy of cancer? Nat Rev Immnol 2002;2:175–84.
27. Balkwill F. Cancer and the chemokine network. Nat Rev Cancer 2004;4:540–50.
28. Dell'Agnola C, Biragyn A. Clinical utilization of chemokines to combat cancer: the double-edged sword. Expert Rev Vaccines 2007;6: 267–83.
29. Tsuchiyama T, Nakamoto Y, Sakai Y, Mukaida N, Kaneko S. Optimal amount of monocyte chemoattractant protein-1 enhances antitumor effects of suicide gene therapy against hepatocellular carcinoma by M1 macrophage activation. Cancer Sci 2008;99: 2075–82.
30. Nakashima E, Ova A, Kubota YA. A candidate for cancer gene therapy: MIP-1α gene transfer to an adenocarcinoma cell line reduced tumorigenesity and induced protective immunity in immunocompetent mice. Pharm Res 1996;13:1896–901.
31. Geissmann F, Manz MG, Jung S, Sieweke MH, Merad M, Ley K. Development of monocytes, macrophages, and dendritic cells. Science 2010;327:656–61.
32. Randolph GJ, Ochando J, Partida-Sánchez S. Migration of dendritic cell subsets and their precursors. Annu Rev Immunol 2008;26: 293–316.
33. López-Bravo M, Ardavín C. *In vivo* induction of immune responses to pathogens by conventional dendritic cells. Immunity 2008;29: 343–51.
34. Murdoch C, Muthana M, Coffelt SB, Lewis CE. The role of myeloid cells in the promotion of tumor angiogenesis. Nat Rev Cancer 2008; 8:618–31.
35. Azenshtein E, Luboshits G, Shina S, et al. The CC chemokine RANTES in breast carcinoma progression: regulation of expression and potential mechanism of promalignant activity. Cancer Res 2002; 62:1093–102.
36. Nesbit M, Schaider H, Miller TH, Herlyn M. Low-level monocyte chemoattractant protein-1 stimulation of monocytes leads to tumor formation in nontumorigenic melanoma cells. J Immunol 2001;166: 6483–90.
37. Obeid M, Tesniere A, Ghiringhelli F, et al. Calreticulin exposure dictates the immunogenicity of cancer cell death. Nat Med 2007; 13:54–61.
38. Casares N, Pequignot MO, Tesniere A, et al. Caspase-dependent immunogenicity of doxorubicin-induced tumor cell death. J Exp Med 2005;202:1691–701.
39. Apetoh L, Ghiringhelli F, Tesniere A, et al. Toll-like receptor 4-dependent contribution of the immune system to anticancer chemotherapy and radiotherapy. Nat Med 2007;13:1050–9.
40. Reits EA, Hodge JW, Herberts CA, et al. Radiation modulates the peptide repertoire, enhances MHC class I expression, and induces successful antitumor immunotherapy. J Exp Med 2006;203: 1259–71.
41. Schueller G, Kettenbach J, Sedivy R, et al. Heat shock protein expression induced by percutaneous radiofrequency ablation of hepatocellular carcinoma *in vivo*. Int J Oncol 2004;24:609–13.
42. Nikfarjam M, Muralidharan V, Su K, Malcontenti-Wilson C, Christophi C. Patterns of heat shock protein (HSP70) expression and Kupffer cell activity following thermal ablation of liver and colorectal liver metastasis. Int J Hyperthermia 2005;21:319–32.

THE JOURNAL OF GENE MEDICINE
*J Gene Med* 2010;**12**: 1002–1013.
Published online in Wiley Online Library (wileyonlinelibrary.com) **DOI:** 10.1002/jgm.1528

**RESEARCH ARTICLE**

# Prevention of intrahepatic metastasis of liver cancer by suicide gene therapy and chemokine ligand 2/monocyte chemoattractant protein-1 delivery in mice

Kaheita Kakinoki[1]
Yasunari Nakamoto[1]
Takashi Kagaya[1]
Tomoya Tsuchiyama[1]
Yoshio Sakai[1]
Tohru Nakahama[1]
Naofumi Mukaida[2]
Shuichi Kaneko[1]*

[1]*Disease Control and Homeostasis, Graduate School of Medical Science, Kanazawa University, Kanazawa, Japan*

[2]*Division of Molecular Bioregulation, Cancer Research Institute, Kanazawa University, Kanazawa, Japan*

*Correspondence to:
Shuichi Kaneko, Disease Control and Homeostasis, Graduate School of Medical Science, Kanazawa University, 13-1 Takara-machi, Kanazawa 920-8641, Japan
E-mail: skaneko@m-kanazawa.jp

*Received: 22 June 2010*
*Revised: 28 October 2010*
*Accepted: 5 November 2010*

## Abstract

**Background** The prognosis of patients with hepatocellular carcinoma (HCC) remains poor, largely as a result of intrahepatic metastasis. Using a mouse model of intrahepatic metastasis, we investigated whether chemokine ligand 2/monocyte chemoattractant protein-1 (CCL2/MCP-1) could potentiate the antitumor effects of the herpes simplex virus thymidine kinase/ganciclovir (HSV-tk/GCV) system.

**Methods** Mouse hepatoma cells infected with recombinant adenovirus vectors expressing HSV-tk, CCL2/MCP-1 and LacZ at multiplicities of infection of Ad-tk/Ad-MCP1 = 3/0.03 ($T/M^{Low}$), 3/3 ($T/M^{High}$) and Ad-tk/Ad-LacZ = 3/3 (T/L) were injected into BALB/c mice.

**Results** Intrahepatic tumor growth was significantly lower in $T/M^{Low}$ mice. By contrast, no tumor suppression was observed in $T/M^{High}$ mice. The tumor-specific cytolytic activities of splenocytes from $T/M^{Low}$ and $T/M^{High}$ mice were comparable. Immunohistochemical analysis of liver tissues showed similar infiltration by Mac-$1^+$ and T cells in these animals, whereas the proportions of classical activated (M1) monocytes/macrophages were significantly higher in $T/M^{Low}$ mice. In addition, interleukin-12 production was elevated in these tissues. Vascular endothelial growth factor-A expression and $CD31^+$ microvessels were increased in $T/M^{High}$ mice.

**Conclusions** Collectively, these results demonstrate that an adequate amount of CCL2/MCP-1, together with the HSV-tk/GCV system, may induce T helper 1-polarized antitumor effects without inducing tumor angiogenesis in the microenvironment of intrahepatic HCC progression. Copyright © 2010 John Wiley & Sons, Ltd.

**Keywords** chemokines; hepatocellular carcinoma; monocytes/macrophages

## Introduction

Primary liver cancer is the fifth most common neoplasm in the world and the third most common cause of cancer-related deaths [1,2]. Despite the development of novel modalities for the treatment of hepatocellular carcinoma (HCC), including transcatheter arterial embolization, percutaneous ablation, surgical resection and liver transplantation, the prognosis of patients with HCC still remains relatively poor. One of the major factors responsible for

these unsatisfactory outcomes is the high frequency of intrahepatic recurrence after curative treatment [1,2]. Intrahepatic recurrence is the result of two mechanisms: intrahepatic metastasis (IM) originating from the primary cancer, and a second primary cancer arising from multicentric carcinogenesis (MC). IM may correlate with early recurrence and poor prognosis, whereas MC is associated with relatively good prognosis [3–5].

To develop novel antitumor strategies for HCC, we have investigated the effectiveness of immune gene therapy using suicide genes and chemokine molecules, including chemokine ligand 2/monocyte chemoattractant protein-1 (CCL2/MCP-1) [6–8]. CCL2/MCP-1 is a chemokine that regulates the recruitment of monocytes/macrophages to inflammatory sites and tumor tissues, as well as their activation, including lysosomal enzyme release and tumoricidal activity, and is functional in both mice and humans [9]. Transfectant-derived CCL2/MCP-1 has been found to successfully recruit monocytes into tumor tissue [10,11]. We recently described a combination strategy for the treatment of HCC, consisting of the herpes simplex virus thymidine kinase/ganciclovir (HSV-tk/GCV) system and CCL2/MCP-1 gene delivery. We found that adenovirally delivered CCL2/MCP-1 enhanced the antitumor effects of the HSV-tk/GCV system by activating innate immune responses involving monocytes/macrophages, as well as demonstrating prolonged efficacy mediated by natural killer cells [6–8]. These experiments were performed in athymic nude mice, deficient in acquired immune responses, subcutaneously transplanted with HCC.

In the present study, we have used a liver metastasis model, in which tumor cells were infused through the portal vein (PV), to investigate whether CCL2/MCP-1 gene delivery could potentiate the antitumor effects of the suicide gene system. The results obtained indicate that the antitumor effects of the suicide gene are enhanced by codelivery of an adequate amount of CCL2/MCP-1. These antitumor effects were associated with the recruitment of monocytes/macrophages and T cells, T helper 1 (Th1) cytokine gene expression and the induction of splenocyte cytolytic activity. These findings indicate that CCL2/MCP-1 has an immunomodulatory effect on suicide gene therapy for HCC by orchestrating the innate and acquired immune responses.

# Materials and methods

## Animals

Male BALB/cA Jcl mice, 6–8 weeks of age, were obtained from CLEA Japan Inc. (Tokyo, Japan), maintained at constant room temperature (25 °C) and provided with free access to standard diet and tap water throughout, in accordance with institutional guidelines.

## Cell lines and cell culture

The mouse HCC cell line BNL 1ME A.7R.1 (BNL) and the mouse colon cancer cell line colon 26 clone 20 (CT 26), derived from BALB/c mice (H-2d), were cultured in Dulbecco's modified Eagle's medium supplemented with 10% heat-inactivated (30 min at 56 °C) fetal bovine serum (FBS), non-essential amino acids, sodium pyruvate, HEPES buffer, 2 mM glutamate, 1 mM penicillin/streptomycin and 0.2 mM gentamicin (Gibco, Long Island, NY, USA) at 37 °C in 5% $CO_2$.

## Recombinant adenovirus vectors

The following replication-defective adenovirus vectors, driven by the CAG promoter [12], were prepared by recombinant DNA technology: Ad-tk, which expresses the HSV-tk gene; Ad-MCP1, which expresses the human CCL2/MCP-1 gene; and Ad-LacZ, which expresses the LacZ gene [13] (Figure 1A). Each recombinant adenovirus vector was purified and titered according to protocols supplied by the manufacturer (Takara, Ootsu, Japan). Briefly, each gene fragment (i.e. HSV-tk, CCL2/MCP-1 and LacZ) was excised from its respective insert-containing pBluescript vector and inserted into the cosmid pAxCA-wt (Takara, Ootsu, Japan), which contains essentially the full-length adenovirus type 5 genome apart from the E1 and E3 regions, thus generating the pAxCA gene (Figure 1A). The recombinant adenovirus vectors (rAds) were generated by transfecting 293 cells with pAxCA-gene and adenovirus 5-dlX DNA-terminal protein complex. These rAds were propagated in 293 cells [14], and viral stocks were prepared by standard protocols [15]. The titers of rAds were determined by the 50% tissue culture infectious dose ($TCID_{50}$) method [16].

## Enzyme-linked immunosorbent assay (ELISA) for CCL2/MCP-1

Aliquots of $2.5 \times 10^4$ BNL cells were seeded in 3.0 ml of culture media in six-well tissue culture plate. After 24 h, the cells were infected with Ad-MCP1 and Ad-MCP1, together with Ad-tk, at various multiplicities of infections (MOIs). After 24 h, the media were collected from the wells, and the concentrations of CCL2/MCP-1 were determined by ELISA. Briefly, each well of a 96-well microtiter plate (Nalgene, Rochester, NY, USA) was coated with 0.05 M carbonate buffer (pH 9.6) containing monoclonal anti-human CCL2/MCP-1 antibody (ME 6.1; 1 μg/ml) overnight at 4 °C. After washing with phosphate-buffered saline (PBS) containing 0.05% Tween 20, the plates were blocked with PBS containing 1% bovine serum albumin for 1 h at 37 °C. Diluted culture medium or various concentrations of recombinant CCL2/MCP-1 were added to duplicate wells and incubated for 2 h at 37 °C. The plates were washed, incubated with rabbit anti-CCL2/MCP-1 antibodies (1 μg/ml) for 2 h at 37 °C,

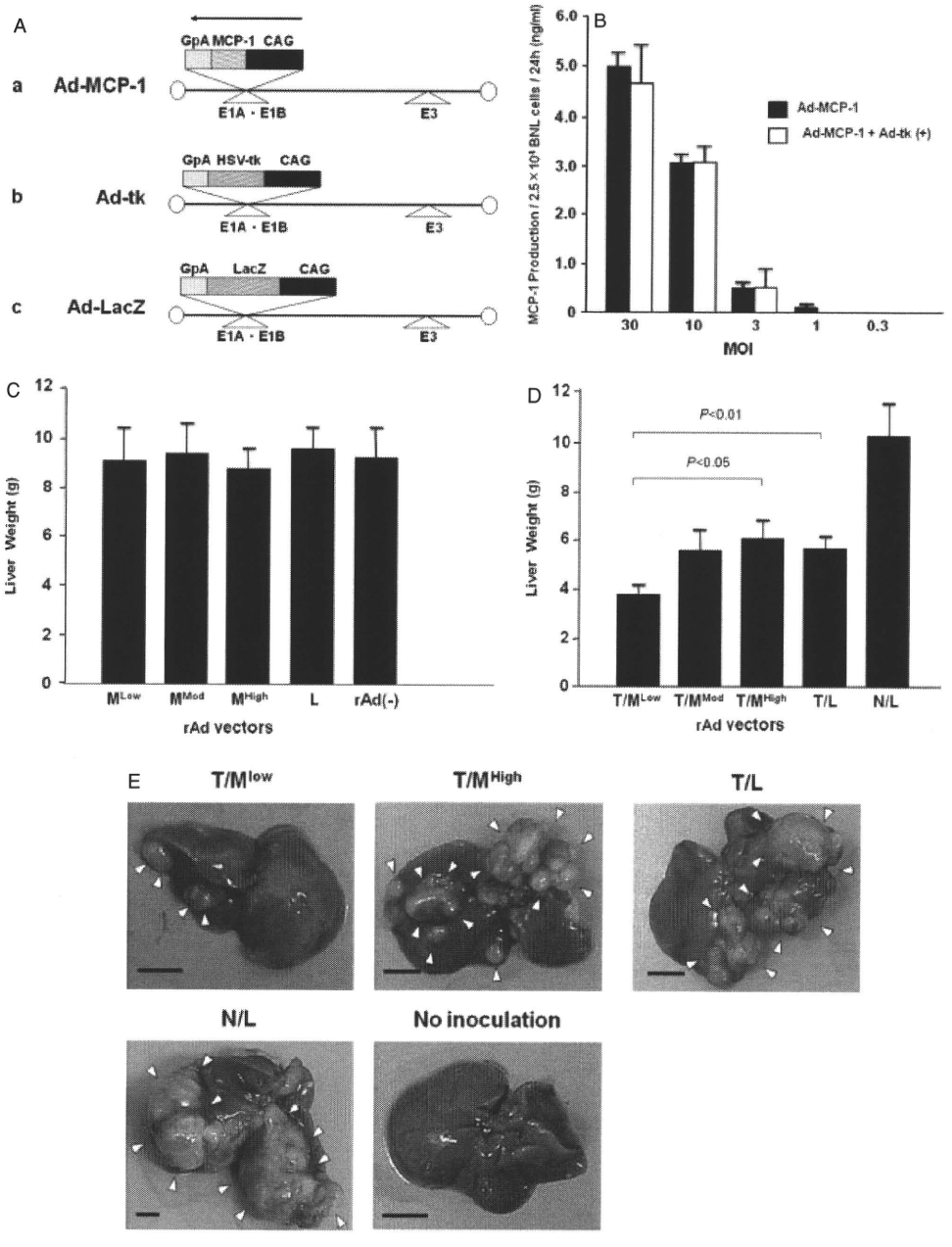


Figure 1. CCL2/MCP-1 production and antitumor effects of rAds. (A) Schematic representation of rAds expressing each gene under the control of a CAG promoter. (a) Ad-MCP1 expressing CCL2/MCP-1. (b) Ad-tk expressing HSV-tk. (c) Ad-LacZ expressing $\beta$-galactosidase gene (LacZ). Solid lines indicate the rAd genome, and the open triangle below each rAd genome represents the deletion of adenovirus early regions. The arrow shows the orientation of transcription. GpA, rabbit $\beta$-globin (A) site; CAG, CAG promoter. (B) Production of CCL2/MCP-1 by BNL cells infected with rAds at various MOIs. The CCL2/MCP-1 concentrations in culture supernatants were determined by ELISA. Data shown are the mean $\pm$ SE of three independent results. (C) Liver weight following transfer of BNL cells infected with Ad-MCP1, Ad-LacZ or PBS (−). Each mouse was injected via the PV with $1 \times 10^6$ BNL cells infected with Ad-MCP1 at various MOIs: 0.03 ($M^{Low}$), 0.3 ($M^{Mod}$) and 3 ($M^{High}$), and Ad-LacZ at the MOI of 3 (L), and the whole livers were weighed on day 21. (D) CCL2/MCP-1 enhancement of the antitumor effects of the HSV-tk/GCV system against intrahepatic cancer cells. Each mouse was injected via the PV with BNL cells ($1 \times 10^6$) infected with Ad-tk, Ad-MCP1 and Ad-LacZ at various MOIs: Ad-tk/Ad-MCP1 = 3/0.03 ($T/M^{Low}$), 3/0.3 ($T/M^{Mod}$) and 3/3 ($T/M^{High}$); Ad-tk/Ad-LacZ = 3/3 (T/L); and Ad-LacZ = 6 (N/L), and the whole livers were weighed on day 21. (E) The macroscopic views of hepatic tumors (open arrowheads) in mice. Tumor growth was markedly suppressed in $T/M^{Low}$ mice. Scale bars = 10 mm

washed again and incubated with alkaline phosphatase-conjugated goat anti-rabbit antibody (1:12 000; Tago, Burlingame, CA, USA) for 2 h at 37 °C. The plates were washed, aliquots of 1 mg/ml *p*-nitrophenylphosphate (Sigma, St Louis, MO, USA) in 1 M diethanolamine (pH 9.8) supplemented with 0.5 mM $MgCl_2$ were added to the wells, and the plates were incubated for 40 min at room temperature. After addition of 1 M NaCl, the optical density (at 405 nm) was assessed using an ELISA plate reader (MTP-120; Corona Electric, Ibaragi, Japan). All experiments were repeated in triplicate.

## Disease model

To evaluate the direct antitumor effect of CCL2/MCP-1, $1 \times 10^7$ BNL cells suspended in 0.5 ml of culture medium were infected *in vitro* with CCL2/MCP-1 at various MOIs: 0.03 ($M^{Low}$), 0.3 ($M^{Mod}$) and 3 ($M^{High}$); Ad-LacZ at an MOI of 3 (L); or PBS (−). The cells were harvested after 30 min of incubation at 37 °C. BALB/c mice were anesthetized by intraperitoneal injection with sodium pentobarbital (Somnopentyl, Schering-Plough Animal Health Corporation, Kenilworth, NJ, USA), and laparotomy was performed. Each mouse was injected with $1 \times 10^6$ adenovirus-infected BNL cells in a volume of 0.2 ml PBS containing 2% FBS or 0.2 ml PBS (−) via PV on day 0. The mice were sacrificed on day 21, and their liver tissues were weighed.

To determine whether CCL2/MCP-1 can enhance the antitumor effects of the HSV-tk/GCV system, BNL cells were infected with Ad-tk, Ad-MCP1 and Ad-LacZ at various MOIs: Ad-tk/Ad-MCP1 = 3/0.03 ($T/M^{Low}$), 3/0.3 ($T/M^{Mod}$) and 3/3 ($T/M^{High}$); Ad-tk/Ad-LacZ = 3/3 (T/L); and Ad-LacZ = 6 (N/L). BALB/c mice were anesthetized and each was injected via portal vein with $1 \times 10^6$ adenovirus-infected BNL cells on day 0, followed by intraperitoneal injection of 75 mg/kg/day ganciclovir on days 2–6. The mice were sacrificed on day 21, and the livers were removed and weighed. Additionally, in another series of experiments, the livers removed from the mice on days 1, 3, 7 and 14 were processed for immunohistochemistry and real-time quantitative reverse transcriptase-polymerase chain reaction (RT-PCR). Simultaneously, their splenocytes were tested for cytolytic activity against $^{51}Cr$-labeled BNL cells.

## Histopathological and immunohistochemical analysis

Liver sections were fixed in 10% zinc-buffered formalin and stained with hematoxylin and eosin (H&E). For histological evaluation, mouse livers were harvested, embedded in tissue-Tek® OCT embedding medium (Sakura Finetek, Torrance, CA, USA) and stored at −80 °C until use, except those stained for CD31 (Abcam, Cambridge, MA, USA), arginase I (Arg-I; BD Biosciences, Franklin Lakes, NJ, USA) and inducible nitric oxide synthase (iNOS; Thermo Fisher Scientific, Fremont, CA, USA). Cryostat sections of frozen tissues were fixed in cold acetone for 10 min and rinsed three times with PBS. The tissue samples used for CD31, iNOS and Arg-I staining were fixed in 10% phosphate-buffered formalin and embedded in paraffin. Following blocking of nonspecific tissue avidin and biotin with a blocking kit (Vector Laboratories, Burlingame, CA, USA), the slides were incubated with biotin-conjugated monoclonal antibody against Mac-1 (CD11b), CD4, CD8 (PharMingen, San Jose, CA, USA) or Arg-I or polyclonal antiserum against CD31 or iNOS for 30 min at room temperature. Biotin-conjugated rat IgG2b, kappa was used as the negative control. The reaction was visualized using a Vectastain® ABC Standard Kit (Vector Laboratories), followed by counterstaining with hematoxylin.

## Real-time quantitative RT-PCR

The Frozen liver specimens containing necrotic liver tissues or tumor tissues were broken into fine pieces and total RNA was extracted from liver tissues using a ToTALLY RNA® kit (Ambion, Austin, TX, USA) in accordance with the manufacturer's instructions. Total RNA (1 μg) was reverse transcribed into cDNA using a SuperScript® first-strand synthesis system for RT-PCR (Invitrogen, Carlsbad, CA, USA). The first strand cDNA was used for real-time quantitative PCR using the ABI PRISM 7900 (Applied Biosystems, Foster City, CA, USA) with TaqMan® Master Mix (Applied Biosystems), and primers and probes for interleukin (IL)-4, IL-10, IL-12, IL-18, interferon (IFN)$\gamma$, vascular endolthelial growth factor (VEGF)-A and 18S ribosome (sequences available on request from the authors) (Applied Biosystems). The expression of cytokine mRNA in each sample was normalized relative to that of 18S ribosome mRNA.

## Cytotoxic T lymphocyte assay ($^{51}Cr$ release assay)

The cytolytic activity of mouse spleen cells was assessed by a $^{51}Cr$ release assay, as described previously [17]. Briefly, each treated mouse was sacrificed on day 14, splenocytes were harvested aseptically and mashed in alpha-minimal essential medium (MEM) medium (Gibco) with 10% FBS, and suspensions of single spleen cells were prepared. Spleen cells were cultured with mitomycin C (MMC; Sigma) (400 μg/4 ml, 1 mg/ml in HBSS) treated BNL or CT26 cells in complete alpha-MEM medium containing 10% FBS and 2.5% EL-4 culture supernatant (a source of T cell growth factor) for 5 days. Target cells consisted of $3 \times 10^5$ BNL cells labeled with 0.3 mCi $Na_2{}^{51}CrO_4$ (NEN Life Science Products, Boston, MA, USA) at 37 °C for 1 h. Effector spleen cells were incubated with $5 \times 10^3$ target cells in 96-well plates at various effector/target ratios for 4 h at 37 °C, and the $^{51}Cr$ released into the culture supernatants was quantified by scintillation

counting. Percent specific cytotoxicity was calculated according to the equation: [100 × (experimental release − spontaneous release)/(maximum release − spontaneous release)]. Spontaneous release was defined as the $^{51}Cr$ in the supernatant of target cells incubated for 4 h, and maximum release was defined as $^{51}Cr$ in the supernatant of target cells treated with 2% Triton-X. Experiments were performed three times and the results expressed as the mean ± SE. Tumor specificity was determined based on differences between BNL and CT 26 cells. All results presented are the means of triplicate assays.

# Results

## CCL2/MCP-1 production of recombinant adenoviruses *in vitro*

The production of CCL2/MCP-1 was evaluated by measuring the concentrations in culture media of BNL cells infected with varying MOIs of Ad-MCP1 and Ad-MCP1 plus Ad-tk by ELISA (Figure 1B). The production of CCL2/MCP-1 by cells infected with Ad-MCP1 increased in proportion to the MOI. Importantly, its production by Ad-MCP1 infected cells was not changed when these cells were further infected with Ad-tk (Ad-MCP1 plus Ad-tk), indicating that CCL2/MCP-1 production by Ad-MCP1 was not influenced by coinfection with Ad-tk in BNL cells. In addition, the functional properties of CCL2/MCP-1 produced by this rAd were defined previously [6–8].

## Intrahepatic tumor development following transfer of HCC cells infected with recombinant adenoviruses

To evaluate the direct antitumor effect of CCL2/MCP-1 in an immunocompetent mouse model of IM, mice were injected via the PV with BNL cells infected with Ad-MCP1 or Ad-LacZ at various MOIs (Figure 1C). When whole livers were weighed on day 21, the weights of $M^{Low}$ ($n = 4$), $M^{Mod}$ ($n = 7$) and $M^{High}$ ($n = 6$) were comparable to those of L ($n = 4$) mice, indicating that delivery of CCL2/MCP-1 gene did not promote or suppress the growth of tumor cells in this model.

To determine whether CCL2/MCP-1 gene delivery can potentiate the antitumor effects of the HSV-tk/GCV system, mice were injected with BNL cells infected with rAds (Ad-tk, Ad-MCP1 and Ad-LacZ) at various MOIs as described in the Materials and methods. Whole livers were weighed on day 21, and the weights of $T/M^{Low}$ ($n = 14$), $T/M^{Mod}$ ($n = 12$), $T/M^{High}$ ($n = 11$) and T/L ($n = 10$) mice were compared with those of N/L ($n = 10$) mice. The reduction in liver weight for the T/L mice was a result of the HSV-tk/GCV system alone, and those for $T/M^{Low}$, $T/M^{Mod}$ and $T/M^{High}$ were a result of treatment in combination with CCL2/MCP-1. Mean ± SEM liver weight was significantly lower in $T/M^{Low}$ mice than in T/L mice (3.91 ± 0.36 g versus 5.80 ± 0.58 g; $p < 0.01$) (Figures 1D and 1E) as a result of the reduced growth of implanted tumor cells in the former. By contrast, the increase in liver weight was not suppressed in $T/M^{Mod}$ and $T/M^{High}$ mice whose tumor cells had been treated with higher titers of Ad-MCP1. Thus, only low level CCL2/MCP-1 provided additional antitumor effects and these results indicate that delivery of adequate amounts of Ad-MCP1 enhanced the antitumor effects of the HSV-tk/GCV system against intrahepatic tumor cells.

## Serial analysis of liver histology following tumor cell transfer

To monitor the course of tumor development following HCC cell transfer, mouse livers were harvested on days 1, 3, 7 and 14. Livers harvested on day 1 from all groups of mice injected with BNL cells showed multiple white patches on their surfaces. Histologically, hepatocyte degeneration and necrosis were observed in these lesions, suggesting that the reduction of PV flow by transferred tumor cells induced focal ischemic necrosis in the livers (Figure 2, closed arrowheads). Although the extent of necrosis was similar among all groups, inflammatory cell infiltration in the area of necrosis was greater in $T/M^{Low}$, $T/M^{High}$ and T/L than in N/L mice. On day 3, cellular infiltration disappeared, and tumor cell growth was observed in areas surrounding the necrotic regions. On day 7, proliferation of viable tumor cells surrounding the necrosis was seen in the livers of N/L mice, with the necrotic tissues completely replaced by tumor cells. Tumor growth was moderately inhibited in T/L mice and greatly inhibited in $T/M^{Low}$ mice. There was no difference between T/L and $T/M^{High}$ mice (not shown). On day 14, the necrotic areas were almost absorbed in all mice. In N/L mice, the tumor cells grew progressively and the tumor masses became larger. Tumor volume was relatively lower in T/L than in N/L mice, although there was no significant difference between T/L and $T/M^{High}$ mice. The greatest degree of tumor growth inhibition was observed in $T/M^{Low}$ mice (Figure 2).

## Recruitment of immune cells in liver

To evaluate the involvement of immune responses in the CCL2/MCP-1 associated enhancement of the antitumor effects of rAd expressing HSV-tk, we assessed the recruitment of Mac-$1^+$ monocytes/macrophages and $CD4^+$ and $CD8^+$ T lymphocytes immunohistochemically (Figure 3).

$T/M^{Low}$ and $T/M^{High}$ mouse liver tissues harvested on day 1 showed marked infiltration of Mac-$1^+$ cells in the necrotic areas induced by tumor cell injection (Figure 3A). Quantitative morphometric analysis showed that the numbers of Mac-$1^+$ cells were significantly higher in liver tissues of $T/M^{Low}$ and $T/M^{High}$ mice [mean ± SEM of 40 high power (×400) fields of necrotic liver

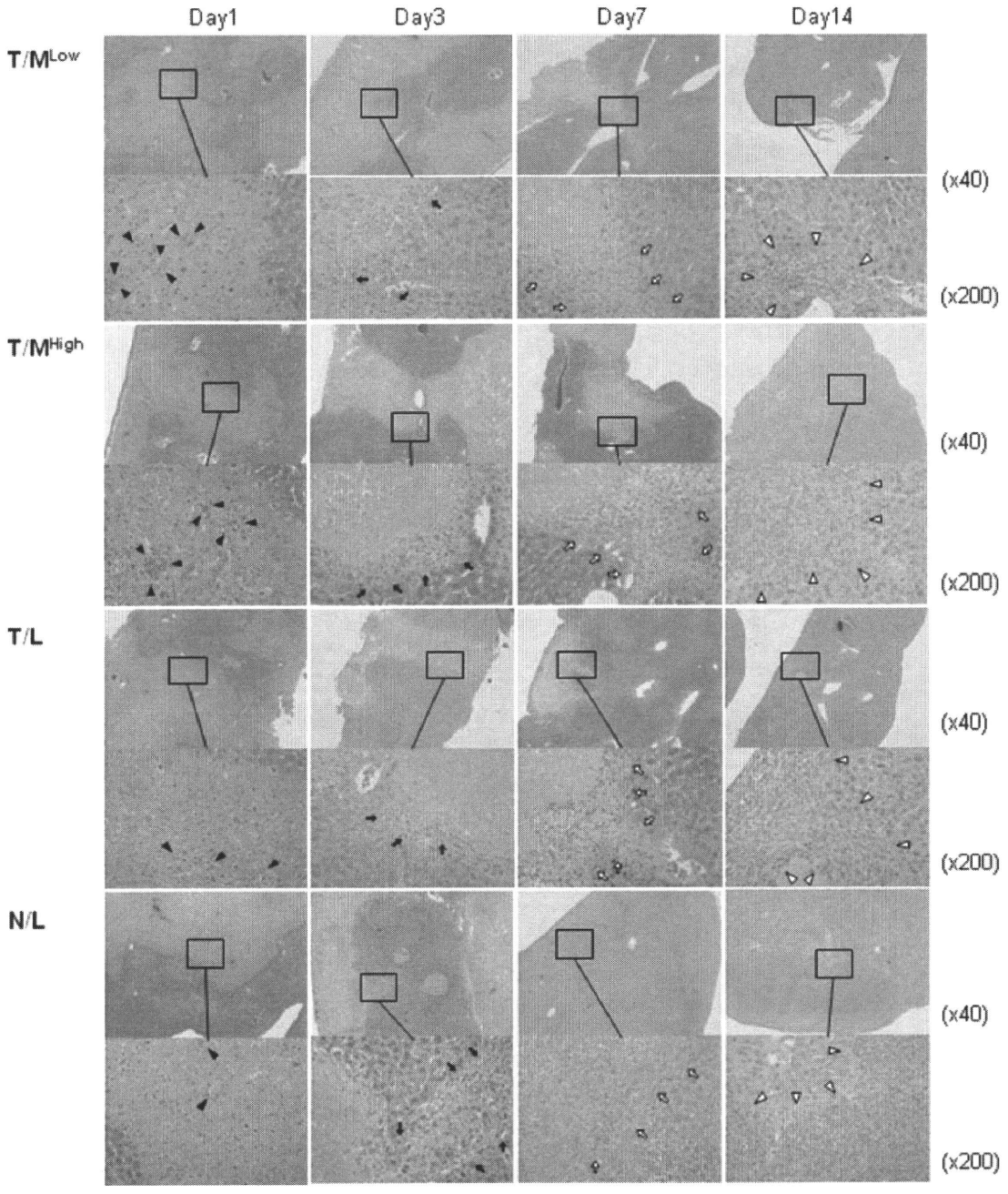


Figure 2. Serial analysis of liver histology following tumor cell transfer. Mouse liver tissues were harvested on days 1, 3, 7 and 14, and stained with H&E. On day 1, all mice injected with BNL cells showed multiple white patches on the liver surface (not shown). Histologically, hepatocyte degeneration and necrosis were observed in these lesions, suggesting that the reduction of PV flow by transferred tumor cells induced focal ischemic necrosis in the livers. The area of necrosis significantly infiltrated with inflammatory cells (closed arrowheads) was higher in $T/M^{Low}$, $T/M^{High}$ and T/L mice than in N/L mice. On day 3, cellular infiltration disappeared and tumor cell growth (closed arrows) was detected in areas surrounding the necrotic regions. On day 7, tumor tissue enlarged and replaced the necrotic areas (open arrows). On day 14, the necrotic areas disappeared and tumor nodules eventually formed (open arrowheads). Original magnifications $\times 40$ and $\times 200$



*J Gene Med* 2010;**12**: 1002–1013.
DOI: 10.1002/jgm

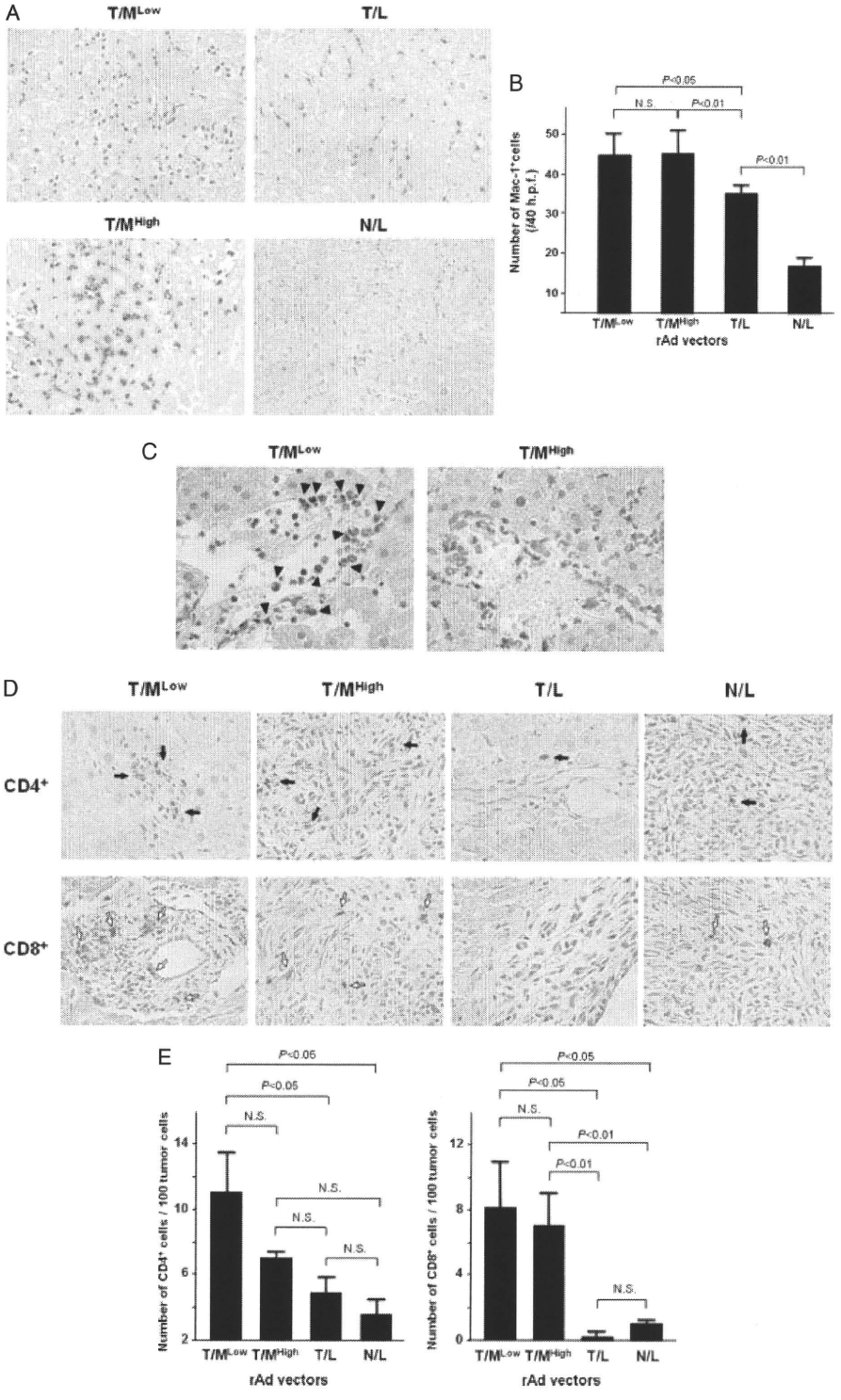


Figure 3. Immunohistochemical evaluation of monocyte/macrophage (A–C) and T cell (D, E) recruitment into liver tissues. (A) Monocyte/macrophage detection using anti-Mac-1 monoclonal antibody. Original magnification ×400. (B) Quantitative morphometric analysis of Mac-1$^+$ cells. (C) Immunohistochemical evaluation of the polarization towards M1 phenotype of recruited monocytes/macrophages using antibody against iNOS (closed arrowheads). (D) CD4$^+$ (closed arrows) and CD8$^+$ (open arrows) T cell detection. Original magnification ×400. (E) Quantitative morphometric analysis of CD4$^+$ and CD8$^+$ T cells

tissues: $46.5 \pm 3.7$ and $46.9 \pm 3.7$; $p < 0.05$ and $p < 0.01$, respectively] compared to T/L mice ($35.2 \pm 2.4$). Macrophages can be activated not only by CCL2/MCP-1, but also by tumor cells treated with Ad-tk [6]. In T/L mice, these cells may induce moderate infiltration of Mac-$1^+$ cells (Figure 3B). These findings indicate that the codelivery of the HSV-tk and CCL2/MCP-1 genes was associated with a higher degree of infiltration of Mac-$1^+$ monocytes/macrophages during the initial period of tumor development. Additionally, to investigate whether the recruited monocytes/macrophages were polarized towards the M1 or M2 phenotype, we performed immunohistochemical analysis using antibodies against iNOS (M1) and Arg-I (M2) [17,18] (Figure 3C). The proportion of iNOS$^+$ (M1 subset) cells among the inflammatory cells was significantly higher in T/M$^{Low}$ than in T/M$^{High}$ mice [mean ± SEM number (per 100 inflammatory cells) of eight high power (×400) fields of necrotic liver tissues: $23.0 \pm 2.7$ and $10.8 \pm 2.5$; $p < 0.01$, respectively]. Arg-I$^+$ (M2 subset) cells were not specifically detected, most likely as a result of the large amounts of the enzyme present in liver tissues.

Similarly, liver tissues obtained on day 14 after HCC cell transfer were immunohistochemically analyzed for immune cell infiltration. In both T/M$^{Low}$ and T/M$^{High}$ mice, the tumor foci were heavily infiltrated by CD4$^+$ and CD8$^+$ T cells (Figure 3D). Quantitative morphometric analysis showed that the numbers of CD4$^+$ and CD8$^+$ T cells were higher in T/M$^{Low}$ [mean ± SEM number (per 100 tumor cells) of eight high power (×400) fields of liver tissues: $11.1 \pm 2.5$ and $8.1 \pm 2.7$; $p < 0.05$ and $p < 0.05$, respectively] and T/M$^{High}$ ($7.1 \pm 1.9$ and $7.1 \pm 0.7$; not significant and $p < 0.01$, respectively) mice than in T/L mice ($4.8 \pm 1.1$ and $0.3 \pm 0.3$, respectively) (Figure 3E). These results suggest that the antitumor activities in T/M$^{Low}$ mice may be mediated not only by the activation of macrophages during the initial period of tumor development, but also by the induction of T cell-mediated immune responses during later periods.

## Cytokine gene expression in liver

Mice injected with adenovirus-infected HCC cells were sacrificed on day 1 and their liver tissues were analyzed by quantitative real-time RT-PCR for the expression of mRNA encoding the cytokines IL-4, IL-10, IL-12, IL-18 and IFN-$\gamma$. IL-12 mRNA expression was induced to a greater extent in T/M$^{Low}$ mice than in the other groups ($p < 0.05$). IL-18 mRNA expression tended to be high in the mice treated with CCL2/MCP-1, although these differences were not statistically significant (Figure 4). By contrast, IL-4, IL-10 and IFN-$\gamma$ mRNA was not detected in any samples. These data suggest that infiltrating monocytes/macrophages induced by CCL2/MCP-1 may be activated to enhance the Th1-polarized responses that contribute to tumor immunity.

## Microvessels in HCC

CCL2/MCP-1 has been shown to be associated with angiogenesis [19,20]. To understand the basis of the different antitumor effects observed in T/M$^{Low}$ and T/M$^{High}$ mice, we immunohistochemically stained microvessels within HCCs for CD31. We found that CD31$^+$ microvessels were markedly increased in 7-day tumor tissues of T/M$^{High}$ mice relative to T/M$^{Low}$ and T/L mice (Figure 5A). These results suggest that angiogenesis induced by large amounts of CCL2/MCP-1 may contribute to tumor growth in T/M$^{High}$ mice.

## VEGF gene expression in liver

Liver samples harvested on day 3 were analyzed for the expression of VEGF-A mRNA, which encodes an angiogenic factor that may promote tumor growth. Quantitative real-time RT-PCR showed that VEGF-A gene expression was induced to a greater extent in T/M$^{High}$ mice (Figure 5B), suggesting that the CCL2/MCP-1 enhancement of antitumor effects may be offset by VEGF-induced angiogenesis.

## Cytotoxic activities of splenocytes

To assess the cytotoxic activities of immune cells derived from mice injected with adenovirus-infected tumor cells, isolated and pulsed splenocytes were incubated with $^{51}$Cr-labeled BNL cells in a standard 4-h cytotoxicity assay (Figure 6). Induction of cytotoxic T lymphocytes (CTLs) specific for BNL cells was higher in T/M$^{Low}$ and T/M$^{High}$ mice than in T/L (not significant) and N/L ($p < 0.01$) mice, and there was no significance difference between T/M$^{Low}$ and T/M$^{High}$ mice. Because the immunogenicity of viral vectors or transgene products is known to induce the unfavorable host immune responses, the detection of antitumor CTL activities may be influenced by the responses against rAd vector and HSV-tk [21–23]. Especially, CTL responses against HSV-tk appear to be induced in T/L, T/M$^{Low}$ and T/M$^{High}$ mice. Collectively, the data suggest that cytotoxic activity of CTLs may be enhanced by the codelivery of a suicide gene and CCL2/MCP-1, consistent with their *in vivo* enhancement of antitumor effects.

# Discussion

In the present study, we have shown that combination gene therapy, using the HSV-tk/GCV system and CCL2/MCP-1 gene delivery, was effective for the treatment of HCC in a mouse model of IM. Delivery of an adequate amount of CCL2/MCP-1 enhanced the antitumor effects of the HSV-tk/GCV system against intrahepatic tumor cells. Necrotic areas induced by HCC tumor cell injection showed marked infiltration of iNOS$^+$

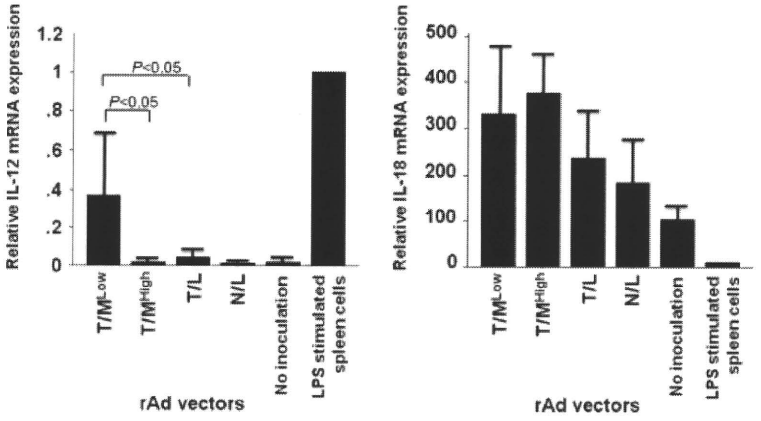


**Figure 4. Real-time quantitative RT-PCR for IL-12 and IL-18 mRNA expression in the liver on day 1. IL-12 gene expression was significantly higher in T/M$^{Low}$ mice than in the other groups ($p < 0.05$)**

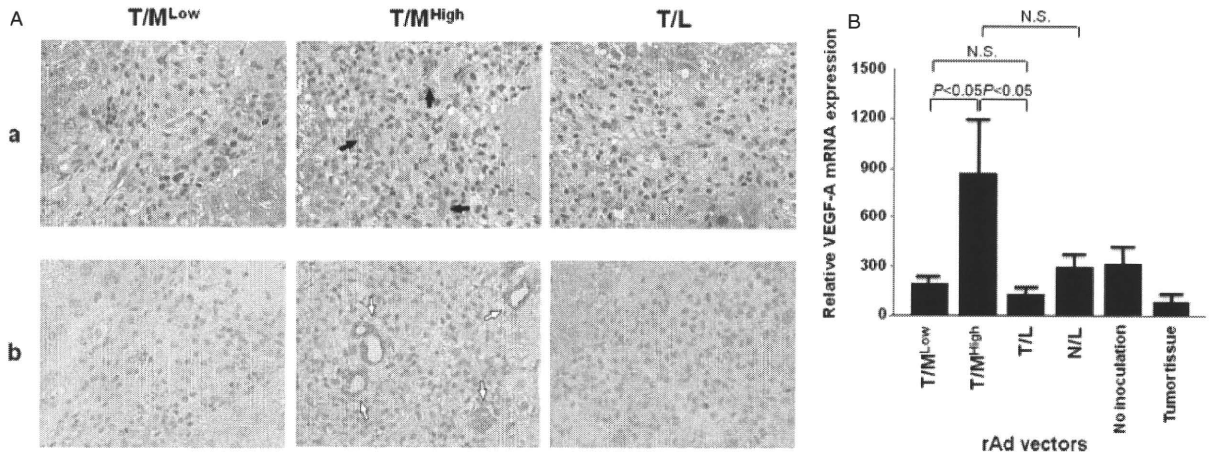


**Figure 5. Evaluation of tumor angiogenesis. (A) Morphometric analysis of microvessels in tumor tissues using H&E staining and CD31 immunohistochemical analysis. (a) Representative H&E stained histological sections of day 7 tumor tissues showing intratumoral microvessels containing red blood cells (closed arrow); endothelial cells were not identified. (b) Representative CD31 immunohistochemical staining showing endothelial cell proliferation in tumor tissues (open arrow). Original magnification ×400. (B) Real-time quantitative RT-PCR for VEGF-A mRNA expression in liver on day 3**

monocytes/macrophages and IL-12 production on day 1, and the tumor foci showed heavy infiltration by CD4$^+$ and CD8$^+$ T cells on day 14. CTLs specific for BNL cells were induced in mice treated with CCL2/MCP-1. By contrast, the expression of the angiogenic factor VEGF-A was significantly increased in mice treated with a large amount of CCL2/MCP-1. Collectively, these results suggest that the delivery of an adequate amount of CCL2/MCP-1, in conjunction with the HSV-tk/GCV system, may display beneficial antitumor effects, preventing the intrahepatic metastasis of HCC cells.

In the development of this model, we injected $1 \times 10^6$ tumor cells infected with recombinant adenoviruses into the portal vein because the injection of fewer cells (e.g. $10^5$) resulted in greatly diminished frequencies of metastasis in the mice. The injection of large numbers of cells, however, may have caused the embolization of cell aggregates in the portal vein, which may have contributed to the induction of ischemic necrosis in the liver tissues. The resultant ischemic death of liver cells may be recognized by immune cells including macrophages, and may result in macrophage activation and the local release of cytokines and chemokines. However, when the mice were injected with control tumor cells (N/L), we observed little infiltration of immune cells, including macrophages and CD4$^+$ and CD8$^+$ T cells, and these mice developed the largest amounts of tumor tissues. These results indicate that any unfavorable effects as a result of ischemic cell death were minimal for the development of intrahepatic metastasis in this model.

This model would be more relevant if ganciclovir treatment was delayed to allow the establishment of tumors. Therefore, we performed the additional experiments with ganciclovir treatment at delayed time point, day 3. Although there was a trend for small amount of MCP-1 to enhance the antitumor effects of the HSV-tk/GCV system, as seen in the experiments on day 1, these differences did not reach statistical significance [T/M$^{Low}$: $7.64 \pm 1.25$ ($n = 10$); T/M$^{Mod}$: $9.24 \pm 0.77$ ($n = 5$); T/M$^{High}$: $9.65 \pm 1.06$ ($n = 8$); T/L: $10.51 \pm 1.79$

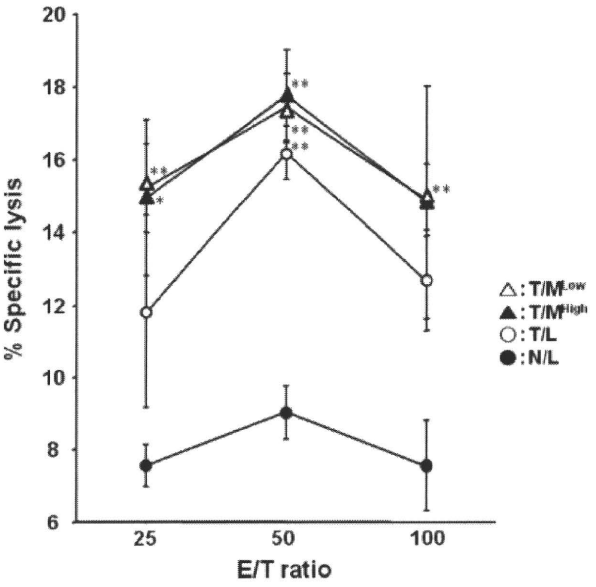


**Figure 6. Cytotoxic activities of splenocytes. Splenocytes harvested on day 14 from individual mice stimulated with MMC-treated BNL cells for 7 days were tested in a standard 4-h cytotoxicity assay with $^{51}$Cr-labeled target (BNL) or control (CT26) cells. $^{*}p < 0.05$ and $^{**}p < 0.01$ compared to N/L mice**

($n = 7$); and N/L: $13.94 \pm 1.16$ ($n = 5$)]. Consequently, the experiment in which ganciclovir was added 3 days after tumor inoculation failed to show a significant antitumor effect. The weakness of this approach may be still the low relevance of the tumor model. The reason is that MCP-1 gene expression by rAds may not be sufficient to enhance antitumor effect at day 3 because the transgene expression gradually diminished with the tumor growth. In our previous studies, MCP-1 production reached peak level on day 2 and decreased after day 3 [6].

Mice treated with small amounts of CCL2/MCP-1 showed enhancement of antitumor effects. The amount of CCL2/MCP-1 delivered, however, was not correlated with monocyte/macrophage accumulation. Although activated monocytes/macrophages are indicative of the potential to eliminate tumor cells [24–26], infiltrating macrophages may enhance tumor growth by secreting growth and angiogenic factors, including VEGF [26–28]. Immunohistochemical analysis of CD31 revealed that microvessels in HCCs were increased in the mice treated with large amounts of CCL2/MCP-1. We also observed a close correlation between the amounts of CCL2/MCP-1 delivered and the levels of VEGF expression. These findings suggest that large amounts of CCL2/MCP-1 may recruit macrophages to induce tumor cell killing and, simultaneously, to facilitate tumor growth, probably by promoting angiogenesis, thus resulting in a reduction of antitumor effects.

CCL2/MCP-1 is a member of the CC chemokine superfamily that promotes the migration of macrophages/monocytes, T lymphocytes, natural killer cells and natural killer T cells not only to sites of inflammation, but also to tumor tissues, which may contribute to the inhibition of tumor growth [29–31]. In addition, the production of CCL2/MCP-1 by tumor tissues has been reported to be associated with favorable prognoses in human pancreatic cancer [31] and neuroblastoma [30]. By contrast, CCL2/MCP-1 may promote tumor growth by chemoattracting tumor-associated macrophages for tumor angiogenesis, or by acting on tumor cells as an autocrine growth factor [29,32,33]. Consistent with this notion, a Japanese study of 135 breast cancer patients found that the women with high levels of tumor-associated CCL2/MCP-1 showed a significantly shorter relapse-free survival [34]. Taken together, the biological and immunological effects of CCL2/MCP-1 appear to vary greatly depending on the diverse microenvironments of cancer tissues.

Two major types of activated macrophages have been described: M1 (classical) and M2 (alternative) [35–38]. M1 macrophages, which play a critical role in the development of antitumor immunity, are characterized by high IL-12 and low IL-10 production. By contrast, M2 macrophages produce reduced amounts of IL-12 but higher levels of Il–10. We found that IL-12 expression was significantly increased in mice treated with a small amount of CCL2/MCP-1 but not in mice treated with a large amount of CCL2/MCP-1, despite the marked infiltration of monocytes/macrophages in the latter. In addition, members of the MCP family have been reported to dose-dependently inhibit IL-12 production by antigen-presenting cells (APCs) [39,40]. Because of the different local concentrations of CCL/MCP-1, we hypothesized that the M1/M2 ratio of recruited monocytes/macrophages may differ in T/M$^{Low}$ and T/M$^{High}$ mice. Indeed, we found that the proportions of M1 cells among infiltrating cells were significantly higher in T/M$^{Low}$ than in T/M$^{High}$ mice. Therefore, M1 monocyte/macrophage polarization may be suppressed in mice treated with large amounts of CCL2/MCP-1, resulting in the reduction of antitumor immunity and the promotion of tumor growth.

Significant tumor infiltration of CD4$^+$ and CD8$^+$ T cells 14 days after transfer was observed in mice treated with the HSV-tk/GCV system plus CCL2/MCP-1. Local secretion of CCL2/MCP-1 by tumor cells may lead to the recruitment and activation of antigen-presenting monocytes/macrophages [41,42]. Once attracted to the tumor tissues, these APCs may ingest pathogenic antigens and transport them to local lymphoid organs, where the antigens are presented to naive T cells, thus establishing a T cell-mediated antitumor response [43]. Tumor growth may thus be impeded by tumor antigen-specific CD4$^+$ and CD8$^+$ T cells.

Although the data obtained in the present study appear to be promising, several problems remain to be solved before clinical application. Our liver metastasis model using a mouse HCC cell line may not be comparable to intrahepatic metastasis of HCC in human patients. However, HCC patients treated by nonsurgical procedures, including percutaneous radiofrequency ablation therapy and transcatheter arterial chemotherapy [44,45], could also be administered rAds to reduce the incidence of

intrahepatic recurrence and metastasis. The present study demonstrated that, in a mouse model, there is a negative impact on tumor development in the presence of a low level of CCL2/MCP-1, whereas high levels of the protein complicate the situation by having a positive impact on tumor growth (i.e. a balance is required). The therapeutic effects may vary with different tumors. The direct correlation between the overexpression of VEGF in tumor cells and tumor angiogenesis has been demonstrated previously [46], and large amount of CCL2/MCP-1 might be less effective in the treatment of hypervascular tumors such as HCC. However, other cancers resistant to anti-angiogenic drug (e.g. pancreatic cancer) [47,48], probably do not need a good blood supply for tumor growth. In the treatment of hypovascular tumors that are resistant to anti-angiogenic drug, CCL2/MCP-1 may enhance the antitumor effects via activation of M1 macrophages.

Additionally, in the present study, we did not perform *in vivo* delivery experiments of the vectors to existing tumors. There would be many complicated factors affecting the delivery of HSV-tk and CCL2/MCP-1 genes in therapeutic approaches [49,50]. Intra-arterial administration of rAds may result in the induction of immunogenicity or cytotoxicity, especially when spread via blood flow. Extremely high-dose rAds have been found to cause severe unexpected side-effects [51]. To overcome these problems, highly tumor-specific promoters may be needed. In our previous studies, human alpha-fetoprotein (AFP) promoters specific for liver cancer cells were used in an immunodeficient nude mouse models [6,52]. A reporter gene was specifically expressed in AFP producing tumors that were xenografted subcutaneously and disseminated in the liver and lung. However, HSV-tk gene expression was not enhanced sufficiently to kill established tumor cells [53] because the transcriptional activity of AFP promoter was relatively low. Furthermore, neither promoters, nor delivery systems were found to be specific for the BNL mouse tumor cell line. Although better methods of tumor-specific gene delivery and expression are needed, the use of *ex vivo* infection techniques has been found to reproduce tumor specific gene expression *in vivo*.

## Conclusions

Although problems with rAds remain to be resolved before clinical application, the results obtained in the present study suggest that a new strategy, consisting of immune gene therapy accompanied by a suicide gene system, can be used to treat HCC and tumors of other lineages.

## Acknowledgements

We thank Akemi Nakano, Yuzu Hasebe and Yui Fujita for their assistance with the histopathological analysis and immunohistochemistry. We are also grateful to Maki Kawamura and Chiharu Minami for providing animal care.

## References

1. Llovet JM, Burroughs A, Bruix J. Hepatocellular carcinoma. *Lancet* 2003; **362:** 1907–1917.
2. Izumi N, Asahina Y, Noguchi O, *et al.* Risk factors for distant recurrence of hepatocellular carcinoma in the liver after complete coagulation by microwave or radiofrequency ablation. *Cancer* 2001; **91:** 949–956.
3. Poon RT, Fan ST, Ng IO, Lo CM, Liu CL, Wong J. Different risk factors and prognosis for early and late intrahepatic recurrence after resection of hepatocellular carcinoma. *Cancer* 2000; **89:** 500–507.
4. Arii S, Monden K, Niwano M, *et al.* Results of surgical treatment for recurrent hepatocellular carcinoma; comparison of outcome among patients with multicentric carcinogenesis, intrahepatic metastasis, and extrahepatic recurrence. *J Hepatobil Pancreat Surg* 1998; **5:** 86–92.
5. Miyata R, Tanimoto A, Wakabayashi G, *et al.* Accuracy of preoperative prediction of microinvasion of portal vein in hepatocellular carcinoma using superparamagnetic iron oxide-enhanced magnetic resonance imaging and computed tomography during hepatic angiography. *J Gastroenterol* 2006; **41:** 987–995.
6. Sakai Y, Kaneko S, Nakamoto Y, Kagaya T, Mukaida N, Kobayashi K. Enhanced anti-tumor effects of herpes simplex virus thymidine kinase/ganciclovir system by code-livering monocyte chemoattractant protein-1 in hepatocellular carcinoma. *Cancer Gene Ther* 2001; **8:** 695–704.
7. Tsuchiyama T, Kaneko S, Nakamoto Y, *et al.* Enhanced antitumor effects of a bicistronic adenovirus vector expressing both herpes simplex virus thymidine kinase and monocyte chemoattractant protein-1 against hepatocellular carcinoma. *Cancer Gene Ther* 2003; **10:** 260–269.
8. Tsuchiyama T, Nakamoto Y, Sakai Y, *et al.* Prolonged, NK cell-mediated antitumor effects of suicide gene therapy combined with monocyte chemoattractant protein-1 against hepatocellular carcinoma. *J Immunol* 2007; **178:** 574–583.
9. Rollins BJ, Sunday ME. Suppression of tumor formation in vivo by expression of the JE gene in malignant cells. *Mol Cell Biol* 1991; **11:** 3125–3131.
10. Hirose K, Hakozaki M, Nyunoya Y, *et al.* Chemokine gene transfection into tumour cells reduced tumorigenicity in nude mice in association with neutrophilic infiltration. *Br J Cancer* 1995; **72:** 708–714.
11. Huang S, Singh RK, Xie K, *et al.* Expression of the JE/MCP-1 gene suppresses metastatic potential in murine colon carcinoma cells. *Cancer Immunol Immunother* 1994; **39:** 231–238.
12. Kanegae Y, Lee G, Sato Y, *et al.* Efficient gene activation in mammalian cells by using recombinant adenovirus expressing site-specific Cre recombinase. *Nucleic Acids Res* 1995; **23:** 3816–3821.
13. Miyake S, Makimura M, Kanegae Y, *et al.* Efficient generation of recombinant adenoviruses using adenovirus DNA-terminal protein complex and a cosmid bearing the full-length virus genome. *Proc Natl Acad Sci USA* 1996; **93:** 1320–1324.
14. Sato Y, Tanaka K, Lee G, *et al.* Enhanced and specific gene expression via tissue-specific production of Cre recombinase using adenovirus vector. *Biochem Biophys Res Commun* 1998; **244:** 455–462.

15. Matthews DA, Russell WC. Adenovirus protein–protein interactions: hexon and protein VI. *J Gen Virol* 1994; **75:** 3365–3374.
16. Kanegae Y, Makimura M, Saito I. A simple and efficient method for purification of infectious recombinant adenovirus. *Jpn J Med Sci Biol* 1994; **47:** 157–166.
17. Benoit M, Desnues B, Mege JL. Macrophage polarization in bacterial infections. *J Immunol* 2008; **181:** 3733–3739.
18. Redente EF, Orlicky DJ, Bouchard RJ, Malkinson AM. Tumor signaling to the bone marrow changes the phenotype of monocytes and pulmonary macrophages during urethane-induced primary lung tumorigenesis in A/J mice. *Am J Pathol* 2007; **170:** 693–708.
19. Salcedo R, Ponce ML, Young HA, *et al.* Human endothelial cells express CCR2 and respond to MCP-1: direct role of MCP-1 in angiogenesis and tumor progression. *Blood* 2000; **96:** 34–40.
20. Koga M, Kai H, Egami K, *et al.* Mutant MCP-1 therapy inhibits tumor angiogenesis and growth of malignant melanoma in mice. *Biochem Biophys Res Commun* 2008; **365:** 279–284.
21. Berger C, Flowers ME, Warren EH, Riddell SR. Analysis of transgene-specific immune responses that limit the in vivo persistence of adoptively transferred HSV-TK-modified donor T cells after allogeneic hematopoietic cell transplantation. *Blood* 2006; **107:** 2294–2302.
22. Raty JK, Lesch HP, Wirth T, Yla-Herttuala S. Improving safety of gene therapy. *Curr Drug Safety* 2008; **3:** 46–53.
23. Schagen FH, Ossevoort M, Toes RE, Hoeben RC. Immune responses against adenoviral vectors and their transgene products: a review of strategies for evasion. *Crit Rev Oncol Hematol* 2004; **50:** 51–70.
24. Bonta IL, Ben-Efraim S. Involvement of inflammatory mediators in macrophage antitumor activity. *J Leukoc Biol* 1993; **54:** 613–626.
25. Hock H, Dorsch M, Kunzendorf U, Qin Z, Diamantstein T, Blankenstein T. Mechanisms of rejection induced by tumor cell-targeted gene transfer of interleukin 2, interleukin 4, interleukin 7, tumor necrosis factor, or interferon gamma. *Proc Natl Acad Sci USA* 1993; **90:** 2774–2778.
26. Mantovani A, Bottazzi B, Colotta F, Sozzani S, Ruco L. The origin and function of tumor-associated macrophages. *Immunol Today* 1992; **13:** 265–270.
27. Leung SY, Wong MP, Chung LP, Chan AS, Yuen ST. Monocyte chemoattractant protein-1 expression and macrophage infiltration in gliomas. *Acta Neuropathol (Berl)* 1997; **93:** 518–527.
28. Sunderkotter C, Steinbrink K, Goebeler M, Bhardwaj R, Sorg C. Macrophages and angiogenesis. *J Leukoc Biol* 1994; **55:** 410–422.
29. Conti I, Rollins BJ. CCL2 (monocyte chemoattractant protein-1) and cancer. *Semin Cancer Biol* 2004; **14:** 149–154.
30. Raffaghello L, Cocco C, Corrias MV, Airoldi I, Pistoia V. Chemokines in neuroectodermal tumour progression and metastasis. *Semin Cancer Biol* 2009; **19:** 97–102.
31. Monti P, Leone BE, Marchesi F, *et al.* The CC chemokine MCP-1/CCL2 in pancreatic cancer progression: regulation of expression and potential mechanisms of antimalignant activity. *Cancer Res* 2003; **63:** 7451–7461.
32. Loberg RD, Ying C, Craig M, Yan L, Snyder LA, Pienta KJ. CCL2 as an important mediator of prostate cancer growth in vivo through the regulation of macrophage infiltration. *Neoplasia (New York)* 2007; **9:** 556–562.
33. Porta C, Subhra Kumar B, Larghi P, Rubino L, Mancino A, Sica A. Tumor promotion by tumor-associated macrophages. *Adv Exp Med Biol* 2007; **604:** 67–86.
34. Ueno T, Toi M, Saji H, *et al.* Significance of macrophage chemoattractant protein-1 in macrophage recruitment, angiogenesis, and survival in human breast cancer. *Clin Cancer Res* 2000; **6:** 3282–3289.
35. Mosser DM. The many faces of macrophage activation. *J Leukoc Biol* 2003; **73:** 209–212.
36. Edwards JP, Zhang X, Frauwirth KA, Mosser DM. Biochemical and functional characterization of three activated macrophage populations. *J Leukoc Biol* 2006; **80:** 1298–1307.
37. Mantovani A, Sica A, Sozzani S, Allavena P, Vecchi A, Locati M. The chemokine system in diverse forms of macrophage activation and polarization. *Trends Immunol* 2004; **25:** 677–66.
38. Gratchev A, Kzhyshkowska J, Kothe K, *et al.* Mphi1 and Mphi2 can be repolarized by Th2 or Th1 cytokines, respectively, and respond to exogenous danger signals. *Immunobiology* 2006; **211:** 473–486.
39. Braun MC, Lahey E, Kelsall BL. Selective suppression of IL-12 production by chemoattractants. *J Immunol* 2000; **164:** 3009–3017.
40. Matsunaga K, Klein TW, Newton C, Friedman H, Yamamoto Y. Legionella pneumophila suppresses interleukin-12 production by macrophages. *Infect Immun* 2001; **69:** 1929–1933.
41. Gu L, Tseng S, Horner RM, Tam C, Loda M, Rollins BJ. Control of TH2 polarization by the chemokine monocyte chemoattractant protein-1. *Nature* 2000; **404:** 407–411.
42. Carr MW, Roth SJ, Luther E, Rose SS, Springer TA. Monocyte chemoattractant protein 1 acts as a T-lymphocyte chemoattractant. *Proc Natl Acad Sci USA* 1994; **91:** 3652–3656.
43. Baggiolini M, Dewald B, Moser B. Human chemokines: an update. *Annu Rev Immunol* 1997; **15:** 675–705.
44. Curley SA. Radiofrequency ablation of malignant liver tumors. *Ann Surg Oncol* 2003; **10:** 338–347.
45. Tung-Ping Poon R, Fan ST, Wong J. Risk factors, prevention, and management of postoperative recurrence after resection of hepatocellular carcinoma. *Ann Surg* 2000; **232:** 10–24.
46. Mise M, Arii S, Higashituji H, *et al.* Clinical significance of vascular endothelial growth factor and basic fibroblast growth factor gene expression in liver tumor. *Hepatology (Baltimore)* 1996; **23:** 455–464.
47. Kindler HL, Niedzwiecki D, Hollis D, *et al.* Gemcitabine plus bevacizumab compared with gemcitabine plus placebo in patients with advanced pancreatic cancer: phase III trial of the Cancer and Leukemia Group B (CALGB 80303). *J Clin Oncol* 2010; **28:** 3617–3622.
48. Philip PA, Benedetti J, Corless CL, *et al.* Phase III study comparing gemcitabine plus cetuximab versus gemcitabine in patients with advanced pancreatic adenocarcinoma: Southwest Oncology Group-directed intergroup trial S0205. *J Clin Oncol* 2010; **28:** 3605–3610.
49. Cassidy J, Schatzlein AG. Tumour-targeted drug and gene delivery: principles and concepts. *Exp Reviews Mol Med* 2004; **6:** 1–17.
50. Yu P, Wang X, Fu YX. Enhanced local delivery with reduced systemic toxicity: delivery, delivery, and delivery. *Gene Ther* 2006; **13:** 1131–1132.
51. Marshall E. Gene therapy death prompts review of adenovirus vector. *Science* 1999; **286:** 2244–2245.
52. Kaneko S, Hallenbeck P, Kotani T, *et al.* Adenovirus-mediated gene therapy of hepatocellular carcinoma using cancer-specific gene expression. *Cancer Res* 1995; **55:** 5283–5287.
53. Sakai Y, Kaneko S, Sato Y, *et al.* Gene therapy for hepatocellular carcinoma using two recombinant adenovirus vectors with alpha-fetoprotein promoter and Cre/lox P system. *J Virol Methods* 2001; **92:** 5–17.

# Mass Reduction by Radiofrequency Ablation Before Hepatic Arterial Infusion Chemotherapy Improved Prognosis for Patients With Huge Hepatocellular Carcinoma and Portal Vein Thrombus

Masashi Hirooka[1]
Yohei Koizumi
Yoshiyasu Kisaka
Masanori Abe
Hidehiro Murakami
Bunzo Matsuura
Yoichi Hiasa
Morikazu Onji

**OBJECTIVE.** The prognosis for patients with advanced large hepatocellular carcinoma (HCC) with portal vein (PV) tumor thrombosis remains poor, and treatment is usually limited to hepatic arterial infusion (HAI) chemotherapy. In this study, we first performed mass reduction using radiofrequency ablation (RFA), followed by HAI chemotherapy. Prognosis after this treatment was evaluated.

**SUBJECTS AND METHODS.** HCC with PV tumor thrombosis was diagnosed in 20 patients between April 2004 and December 2008, and treatment was performed using mass-reduction therapy by RFA before HAI chemotherapy. For comparison, 33 patients treated with HAI chemotherapy without RFA were retrospectively selected as historical control subjects under the same conditions. Prognosis in each group was evaluated.

**RESULTS.** Mass-reduction therapy by RFA combined with HAI chemotherapy achieved complete response in six patients (30%), partial response in 11 patients (55%), stable disease in two patients (10%), and progressive disease in one patient (5%). Among the control subjects, complete response was seen in 0 patients (0%), partial response in 12 patients (33.3%), stable disease in 16 patients (44.4%), and progressive disease in eight patients (22.2%). The cumulative survival rates for those who received the combined therapy at 6, 12, and 24 months were 100%, 89.7%, and 78.8%, respectively. The median survival was 953 days (95% CI, 760–1,102 days). In the control subjects, the cumulative survival rates at 6, 12, and 24 months were 84.9%, 56.1%, and 16.9%, respectively ($p < 0.0001$). No serious adverse events were encountered in either group.

**CONCLUSION.** For patients with huge HCC and PV tumor thrombosis, mass-reduction treatment by RFA before HAI chemotherapy is safe and can improve prognosis.

**Keywords:** hepatic arterial infusion chemotherapy, hepatocellular carcinoma, portal vein tumor thrombosis, radiofrequency ablation

DOI:10.2214/AJR.09.2852

Received April 4, 2009; accepted after revision July 22, 2009.

[1]All authors: Department of Gastroenterology and Metabology, Ehime University Graduate School of Medicine, Shizukawa 454, Toon-shi, Ehime 791-0295, Japan. Address correspondence to Yoichi Hiasa (hiasa@m.ehime-u.ac.jp).

**WEB**
This is a Web exclusive article.

*AJR* 2010; 194:W221–W226

0361–803X/10/1942–W221



The prognosis is very poor for patients with hepatocellular carcinoma (HCC) invading the major branches of the portal vein (PV). PV tumor thrombus is associated with the threat of bleeding of the esophageal varices or hepatic failure. Thus, the patient's quality of life is poor.

In several studies, investigators have reported treatment of advanced HCC with PV tumor thrombosis using conventional treatments such as hepatectomy [1, 2], transcatheter hepatic arterial embolization [3], and chemotherapy [4–7]. With regard to aggressive treatment of HCC with PV tumor thrombosis, no acceptable outcomes have yet been obtained. Hepatic arterial infusion (HAI) chemotherapy has recently been reported to improve response rate and survival [4–6]. Although HAI chemotherapy has been attempted widely, the effectiveness of HAI chemotherapy remains unsatisfactory. Studies have revealed that adjuvant HAI chemotherapy after hepatectomy for HCC with PV tumor thrombosis is very effective [1, 8]. However, hepatectomy for small HCC is considered excessively invasive. Hepatectomy for advanced HCC certainly places a considerable burden on the patient. Conversely, radiofrequency ablation (RFA) is less invasive than hepatectomy. With developments in technique for RFA, large HCC and PV tumor thrombosis also can be treated by RFA [9–12].

We therefore propose a new method for the treatment of advanced HCC—using RFA for mass reduction of the tumor before HAI chemotherapy. The aim of this study was to evaluate the safety of this method and the prognosis of patients treated with this method compared with patients who had undergone conventional HAI chemotherapy without RFA.

## Subjects and Methods

### Patients and Inclusion Criteria

Twenty patients (16 men, four women; mean age, 63.9 ± 7.7 [SD] years) who had been admitted to the Department of Gastroenterology and Metabology of the Ehime University Hospital in Japan between April 2004 and December 2008 were diagnosed with HCC with PV tumor thrombosis. After we had obtained written, informed consent from study participants, mass-reduction therapy by RFA was performed before HAI chemotherapy. This prospective cohort study was conducted in accordance with the Declaration of Helsinki.

The criteria for study inclusion were as follows: first, Eastern Cooperative Oncology Group (ECOG) performance status of 0–2; second, successful implantation of an intraarterial catheter and drug delivery system; third, the existence of a giant nodule < 15 cm in diameter or of spread of tumor to comprise < 50% of the total liver volume; fourth, platelet count of > 70,000/mm$^3$; fifth, granulocyte count of > 2,500/mm$^3$; sixth, creatinine clearance of > 60 mL/h; and, seventh, the absence of extrahepatic metastasis. HCC was diagnosed on the basis of histologic findings; imaging studies; and elevated serum α-fetoprotein level, des-γ-carboxy prothrombin (DCP) level, or both.

Thirty-three patients (30 men, three women; mean age, 62.4 ± 7.8 [SD] years) had been treated using HAI chemotherapy without mass-reduction therapy by RFA between January 2002 and December 2008, and these patients were used as historical control subjects. Informed consent was obtained from all prospective subjects before they participated in the trial but was not obtained for retrospective data from historical control subjects. This study was approved by the ethics committee at Ehime University Hospital.

### Catheter Implantation

Celiac angiography was performed using the femoral approach with the patient under local anesthesia. A 5-French heparin-coated catheter was introduced into the proper or common hepatic artery. The gastroduodenal artery and right gastric artery were occluded with steel coils to prevent gastroduodenal injury from anticancer agents. Aberrant hepatic arteries, if present, were occluded with metallic coils or a 1:1.5 mixture of *N*-butyl cyanoacrylate and iodized oil before treatment of hepatic arterial redistribution [13]. After the catheter was connected to the injection port, the device was implanted in a subcutaneous pocket in a femoral site. Patients received regional chemotherapy via the hepatic artery through a subcutaneously implanted port.

### Treatment Protocol for Chemotherapy

We started the chemotherapy after the patients' complications (i.e., fever, elevation of transaminase level) from RFA had improved. Each patient received subcutaneous pegylated interferon (Peg-Intron, Schering-Plough Pharmaceuticals) and intraarterial infusion of 5-fluorouracil (5-FU Injection 250, Kyowa Hakko). One cycle of treatment lasted 4 weeks. Pegylated interferon (50 μg) was administered subcutaneously on days 1, 8, 15, and 22. Continuous infusion chemotherapy (300 mg/m$^2$/d of 5-fluorouracil) through the proper hepatic artery was administered in weeks 1 and 2 using the implanted drug-delivery system. A 2- or 3-week rest period separated each treatment cycle. All anticancer therapies were discontinued when adverse events reached level 2 according to ECOG classifications. At least two cycles of chemotherapy were performed.

### Mass Reduction by RFA

Before mass-reduction treatment was performed, 15 mg of pentazocine hydrochloride and 25 mg of hydroxyzine hydrochloride were administered intramuscularly. Local anesthesia was induced using 5 mL of 1% lidocaine hydrochloride injected through the skin into the peritoneum along a predetermined puncture line. The radiologist performing the procedure inserted a 20-cm-long 17-gauge radiofrequency electrode equipped with a 2- or 3-cm-long exposed metallic tip (Cool-tip, Valleylab) or expandable needle (LeVeen Needle, Boston Scientific). If the diameter of the tumor was more than 5 cm, a 4-cm expandable needle was selected. The Cool-tip needle was used for the PV tumor thrombosis, in which the tumor had a diameter of less than 5 cm. This single needle also was used for residual lesion after ablating by LeVeen needle according to the protocol noted above. If the lung was obstructing the view of the nodule, 500 mL of saline was injected into the right pleural cavity [14].

Ablation was first performed for the intraparenchymal nodule, then the PV tumor thrombosis was treated. During the treatment of PV tumor thrombosis, RFA was performed first for the main portal branch, followed by ablation for PV tumor thrombosis in the peripheral branches. The electrode needle was inserted into the portal thrombus as close to the major axis of the PV tumor thrombosis as possible. A single needle was used to prevent injury to the major branches of the bile duct or artery. The electrode output was set as low as possible (i.e., < 50 W). If the hyperechoic area was not covered for the PV tumor thrombosis, an ethanol injection was added. Ethanol was injected until hyperechoic change of the target area could be seen. Usually, we injected 4 mL or less of ethanol for each session.

After the treatment, we evaluated the efficacy of RFA using CT. Complete necrosis was achieved for all ablated nodules except nonablated daughter nodules. We decided to perform the additional treatment if the viable portion remained by the time of the CT evaluation.

### Estimation of Therapeutic Effect

Posttreatment evaluation was performed every 3 months. The evaluation mainly comprised periodic sonography; CT; and tests for tumor markers, including α-fetoprotein and DCP, for all patients. Objective response was classified according to ECOG criteria [15].

### Statistical Analysis

Data are expressed as means ± SD. Statistical analysis was performed using the Student's *t* test for unpaired data, contingency table analysis, and the Mann-Whitney *U* test as appropriate. Cumulative survival curves were constructed using the Kaplan-Meier method. Values of $p < 0.05$ were considered to represent statistical significance.

## Results

### The Estimation of RFA

Only the Cool-tip needle was used for 20 cases, and both the Cool-tip needle and LeVeen needle were used for 14 cases. In no case was only the LeVeen needle used. Except tumor diameter, there was no significant difference between the cases treated using only the Cool-tip needle (47.4 ± 14.2 mm) and the cases treated using two needles (65.9 ± 22.1 mm) ($p$ = 0.117). Ethanol injection was performed for four patients. The median volume of ethanol was 3.8 ± 0.3 mL (range, 3.5–4.2 mL). The mean number of RFA electrode punctures in each session was 3.0 ± 1.1 (range, 2–7). We ablated the small daughter nodules if there were two or more.

### Post-RFA Complications

The mean number of ablation sessions was 1.7 ± 0.7 (range, 1–3). Complete necrosis of the PV thrombosis was achieved in 17 patients (85%). No serious adverse events were observed after ablation. No patients displayed liver abscess or bleeding, but all patients showed a transient elevation of aspartate aminotransferase (AST) and alanine aminotransferase (ALT). The maximum values of AST and ALT after mass reduction by RFA were 221 and 251 IU/L, respectively. Elevation of ALT was mild (< 150 IU/L) in 10 patients and moderate (150–600 IU / L) in 10 patients. None of the patients showed severe ALT elevation (> 600 IU/L). The ALT level for all patients had recovered within 1 month after RFA. The median interval between the final

ablation until the start of chemotherapy was 9.1 ± 2.8 days (range, 5–14 days).

*Clinical Response to Combination Therapy*

Table 1 summarizes the characteristics of all the patients and control subjects. All patients completed at least two cycles of chemotherapy after RFA. For patients who displayed a clinical response, we continued chemotherapy until HCC progressed. If complete response was achieved, chemotherapy was stopped after the second cycle. Treatment was stopped after completion of the second cycle in patients with no response because of extended progression of HCC. The mean number of treatment cycles was 3.4 ± 2.2 (range, 2–10).

Among the 20 patients treated with RFA before HAI chemotherapy, six patients (30%) showed complete response; 11 (55%), partial response; two (10%), stable disease; and one (5%), progressive disease. In comparison, the control group showed complete response in 0 patients (0%), partial response in 12 (33.3%), stable disease in 16 (44.4%), and progressive disease in eight (22.2%) (Table 2). Of the 20 patients, six patients had PV tumor thrombosis in the main portal trunk and 14 in the major portal branch (Table 1). The response rate in these six patients who had PV tumor thrombosis in the major portal trunk was not significantly worse (83.3%) than that in the other 14 patients (response rate, 92.8%) ($p = 0.199$).

The response rate was significantly better for the mass-reduction group than for the control subjects ($p < 0.0001$). In four patients (20%), patency of the PV was achieved after combination treatment; in eight patients, partial PV patency was seen. Although the viable lesion in the PV tumor thrombosis had disappeared after treatment in two patients, PV flow did not resume in either patient, and cavernous transformation occurred. In the control group, complete patency of the PV occurred for 0 patients and partial patency, for seven patients. The repatency rate of the PV was significantly better ($p = 0.0016$) in the mass-reduction group than in the control group.

In the mass-reduction group, intrahepatic recurrence after chemotherapy was seen in three patients and extrahepatic recurrence, in five patients. In the control group, intrahepatic and extrahepatic recurrence was noted in eight and three patients, respectively ($p = 0.1016$). In the mass-reduction group, the cumulative survival rates at 6, 12, and 24 months were 100%, 89.7%, and 78.8%, respectively. The median survival time was 953 days (95% CI, 760–1,102 days). In the control group, the cumulative survival rates at 6, 12, and 24 months were 84.9%, 56.1%, and 16.9%, respectively. The median survival time was 352 days (95% CI, 267–407 days).

Overall survival rates were significantly improved for the mass-reduction group compared with control subjects ($p < 0.0001$, Fig. 1). The causes of death were as follows in the mass-reduction group: extension of cancer, nine patients; hepatic failure, none; gastroesophageal bleeding, two patients; and other cause, one patient. In the control group, the causes of death were extension of cancer, 27 patients; hepatic failure, two; gastroesophageal bleeding, one patient; and other cause, one patient ($p = 0.573$). Patients and control subjects died and tumor recurrences were noted during both periods of HAI chemotherapy and after cessation of HAI chemotherapy. The frequency between them was not different statistically.

*Case Presentation*

A 55-year-old man underwent RFA for HCC in January 2006. The largest HCC nodule (6.5 × 6.0 cm) in the right lobe was ablated using a 4.5-cm expandable needle. After mass reduction of the intrahepatic lesion, PV tumor thrombosis in the main and right portal branches was ablated using a single RFA needle. HAI chemotherapy (two cycles) was performed 11 days after the reduction therapy,

**TABLE 1: Patient and Tumor Characteristics**

| Characteristic | Patients Who Received HAI Chemotherapy After RFA ($n = 20$) | Historical Control Subjects ($n = 33$) | $p$ |
|---|---|---|---|
| Sex (no. of patients) | | | 0.26 |
| Male | 16 | 30 | |
| Female | 4 | 3 | |
| Age (y) | | | 0.49 |
| Mean ± SD | 63.9 ± 7.7 | 62.4 ± 7.8 | |
| Cause | | | 0.76 |
| Hepatitis B virus | 5 | 6 | |
| Hepatitis C virus | 14 | 26 | |
| Other[a] | 1 | 1 | |
| Child-Pugh class | | | 0.72 |
| A | 16 | 25 | |
| B | 4 | 8 | |
| Tumor diameter (mm) | | | 0.40 |
| Mean ± SD | 57.3 ± 20.9 | 59.1 ± 28.5 | |
| Extent of PV tumor thrombosis | | | 0.26 |
| Main portal trunk | 6 | 15 | |
| Major portal branch | 14 | 18 | |

Note—HAI = hepatic arterial infusion, RFA = radiofrequency ablation, PV = portal vein.
[a]Non–hepatitis B virus, non–hepatitis C virus.

**TABLE 2: Response to Hepatic Arterial Infusion (HAI) Chemotherapy in Patients Who Underwent Radiofrequency Ablation (RFA) and in Control Subjects Who Did Not**

| Response | Patients Who Received HAI Chemotherapy After RFA ($n = 20$) | Historical Control Subjects ($n = 36$) |
|---|---|---|
| Complete response | 6 | 0 |
| Partial response | 11 | 12 |
| Stable disease | 2 | 16 |
| Progressive disease | 1 | 8 |
| Response rate (%) | 85.0 | 33.3 |
| $p$ | < 0.0001 | |

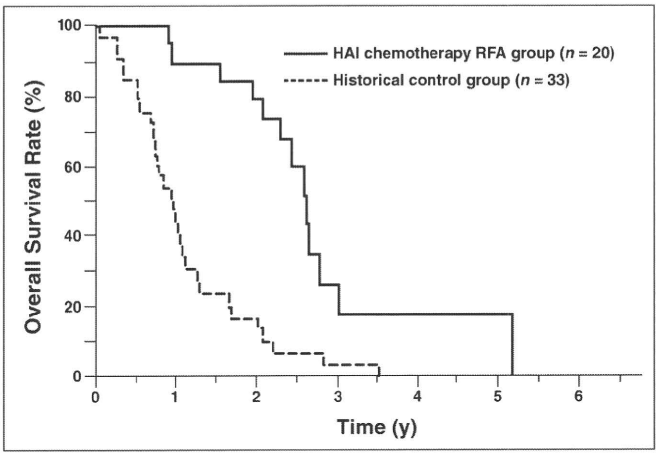


**Fig. 1**—Graph shows cumulative overall survival rates after hepatic arterial infusion (HAI) chemotherapy with and without radiofrequency ablation (RFA). Survival rate was higher for patients who underwent HAI chemotherapy and RFA than for control subjects who underwent HAI chemotherapy only ($p < 0.0001$).

and subsequent CT showed complete necrosis of tumor thrombosis. All tumor marker levels, which had been abnormal before treatment, normalized after RFA and HAI chemotherapy: α-fetoprotein level, from 580.4 to 2.5 ng/mL; α-fetoprotein-L3, from 43.1% to 0%; and DCP, from 598 to 27 mAU/mL (Fig. 2). This patient has undergone follow-up on an outpatient basis, with no evidence of recurrence as of the time of writing.

## Discussion

The prognosis for patients with advanced HCC with PV tumor thrombosis remains poor [16]. The median survival time of HCC patients with PV tumor thrombosis is reportedly approximately 90 days with supportive care [17]. Many therapeutic modalities have been proposed to improve survival rate [1–8], but no standard treatment protocol has yet been defined.

HAI chemotherapy using implanted reservoirs has achieved significant survival benefits for patients with advanced HCC. Ishida et al. [4] reported that HAI chemotherapy with degradable starch microspheres (Spherex, Yakult) achieved an 84.6% response rate, with 1-, 2-, and 3-year survival rates of 100%, 28.9%, and 9.6%, respectively, in all patients and 100%, 33.3%, and 0% in patients with PV tumor thrombosis. The median survival was 22.1 months in all patients and 17.1 months in the six patients with PV tumor thrombosis [4].

If patients have a huge HCC mass with PV tumor thrombosis, response to treatment and survival are worsened [5]. Antitumor effects of those treatments against a huge mass of HCC are considered to be reduced for the following reasons: First, as HCC grows from the moderately differentiated type to the poorly or undifferentiated type, hypovascular changes occur, reducing the ability of anticancer drugs to be delivered to the advanced HCC. Second, huge HCC tumors are often located on the hepatic surface and are often fed by extrahepatic arteries, such as the adrenal or intercostal arteries [18, 19]. Again, this serves to reduce delivery of the anticancer drug from the hepatic artery. Third, in patients with huge HCC, particularly those with PV tumor thrombosis, portal flow is stagnated by invasion of the HCC, reducing liver function [16]. Moreover, delivery of anticancer drugs is again reduced in such cases. Given these factors, assistance by mass-reduction treatment seemed likely to prove useful for patients with huge HCC with PV tumor thrombosis and could improve prognosis compared with HAI chemotherapy monotherapy.

Mass-reduction therapy for patients with huge HCC nodules and PV tumor thrombosis could be compared with transcatheter arterial embolization (TAE) or surgical resection. TAE is a useful method for treating huge nodules. However, TAE requires injection of embolization material through a catheter into the hepatic artery. The response of huge HCC to TAE is often insufficient because of the reasons mentioned earlier. Moreover, if cavernous transformation of the PV has not occurred in cases of HCC with PV tumor thrombosis, parenchymal infarction around HCC can result from TAE, further damaging the liver. TAE is unsuitable for mass-reduction treatment of huge HCC.

Recently, the results of $^{90}$Y therapy for huge HCC have been reported [20]. In Japan, we cannot use $^{90}$Y therapy. Because $^{90}$Y therapy is radiochemoembolization, $^{90}$Y therapy is not suitable for treatment of recurrences. Riaz et al. [20] reported that the rate of complete necrosis by the treatment of $^{90}$Y was only 17% of the tumor for tumors more than 5 cm in diameter, whereas complete necrosis was achieved in all nodules more than 5 cm using our RFA method.

The most curative approach to treating huge HCC with PV tumor thrombosis is surgical resection. However, this option is feasible in only a minority of HCC patients because most patients with huge HCC with PV tumor thrombosis display seriously compromised liver function. Abdominal open surgery is thus too invasive for patients with a limited prognosis. Local ablation therapy for huge HCC has recently been reported [9, 10]. Wider lesions of the liver can be ablated using a multipolar needle and large expandable needle.

For the current study, we performed mass-reduction treatment using RFA and tried to treat PV tumor thrombosis aggressively. In our study, four patients with Child-Pugh grade B cirrhosis showed no deterioration of liver function after ablation of wide HCC lesions. Livraghi et al. [21] reported their first experience of treating PV tumor thrombosis using percutaneous ethanol injection (PEI). Conversely, Giorgio et al. [11] reported treatment of PV tumor thrombosis using RFA.

For the treatment of PV tumor thrombosis, RFA seems more risky than PEI. The risk of bleeding is thought to be higher because the RFA needle that is inserted into the PV is thicker than the PEI needle. Moreover, PVs accompany bile ducts and the hepatic arteries in the liver. If bile ducts and hepatic arteries are injured by RFA for PV tumor thrombosis, severe complications such as biloma, obstructive jaundice, liver abscess, and mass liver infarction can result. We performed RFA for PV tumor thrombosis with a low output (< 50 W), and none of these complications occurred in any of the patients in our study group.

Giorgio et al. [11] reported 10 cases of advanced HCC with PV tumor thrombosis treated using RFA (mean tumor diameter, 4.20 ±

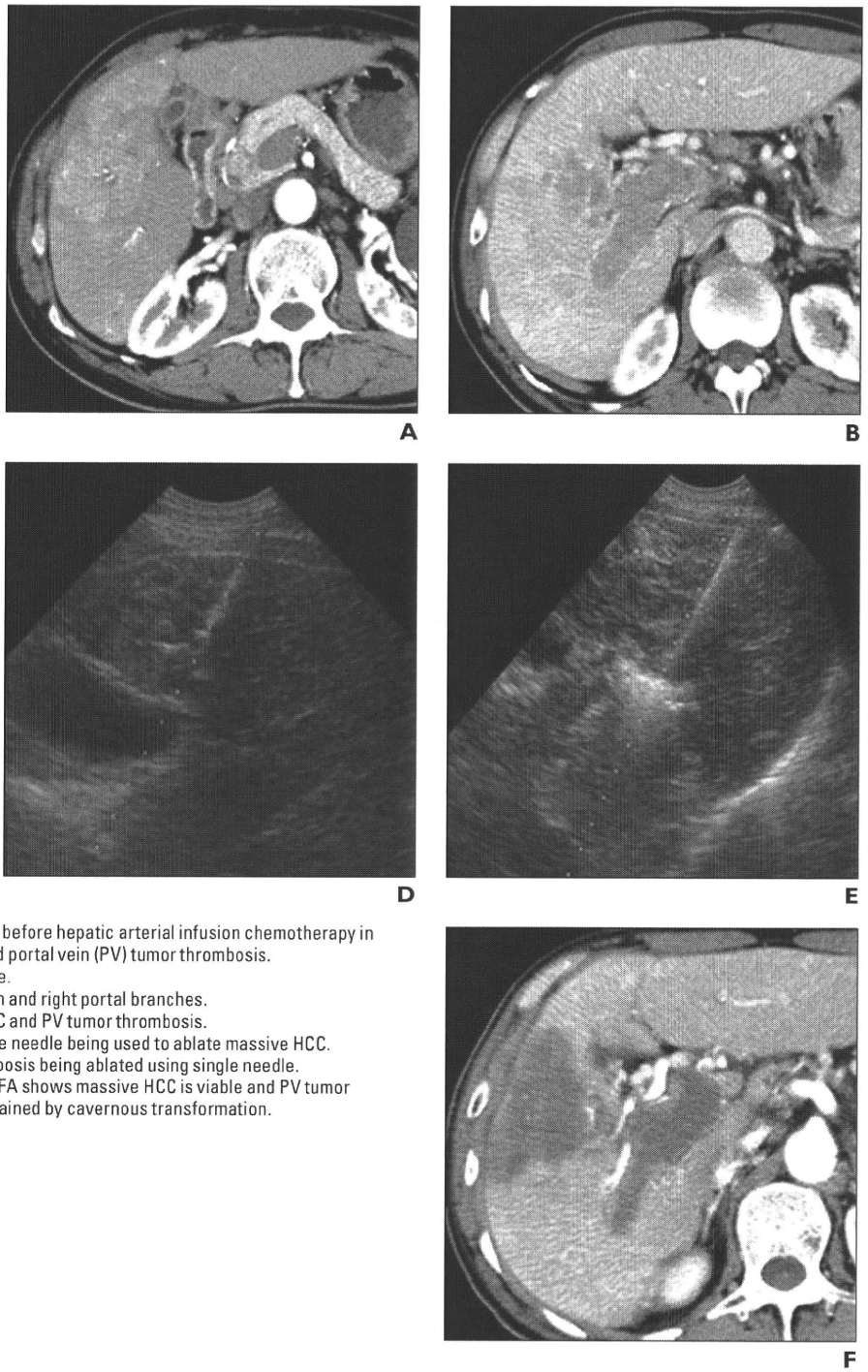


**Fig. 2**—Mass reduction by radiofrequency ablation (RFA) before hepatic arterial infusion chemotherapy in 55-year-old man with hepatocellular carcinoma (HCC) and portal vein (PV) tumor thrombosis.
**A,** Abdominal CT scan shows massive HCC in anterior lobe.
**B,** Abdominal CT scan shows PV tumor thrombosis in main and right portal branches.
**C,** Sonogram obtained before therapy shows massive HCC and PV tumor thrombosis.
**D,** Sonogram obtained during RFA shows wide expandable needle being used to ablate massive HCC.
**E,** Sonogram obtained during RFA shows PV tumor thrombosis being ablated using single needle.
**F,** CT scan obtained after chemotherapy combined with RFA shows massive HCC is viable and PV tumor thrombosis has disappeared. Portal blood flow was maintained by cavernous transformation.

0.36 cm; range, 3.8–4.9 cm). Although the grade of HCC was more serious in our study, our results in terms of survival time (6-, 12-, and 24-month rates of 100%, 89.7%, and 78.8%, respectively) were also good. In four cases in which ablation by RFA was insufficient, we performed PEI for the treatment of PV tumor thrombosis. In all four patients, complete PV flow resumed (Fig. 3).

In some patients, the RFA needle may not reach the far side of the liver where PV tumor thrombosis has expanded to the superior mesenteric vein or splenic vein. Fortunately, we did not encounter any such cases in this study. However, radiotherapy should be considered in such cases.

The effects of radiation associated with mass-reduction treatment and HAI chemotherapy need to be evaluated in a future study. More or less arterial–portal shunting was noted by angiography in all patients who had the PV tumor thrombosis. Our results of the treatment in the patients who had arterial–portal shunting was not bad, indicating that the arterial–portal shunting might not induce the attenuation of the effect of chemotherapy.

In conclusion, we propose a less invasive combined technique using mass-reduction